An Approach to Bridge Inspection Using 3D Laser Scanners and Digital Photographs

By

Muhammad Shumail Farooq

Submitted to the graduate degree program in Civil Engineering and the Graduate Faculty of the University of Kansas in partial fulfillment of the requirements for the degree of Master of Science.

_____

Chair: Daniel Tran Ph. D.

_____

Brian Lines Ph. D.

_____

Michael Panethiere P.E.

Date Defended: 23 May 2017

The Thesis Committee for Muhammad Shumail Farooq

certifies that this is the approved version of the following thesis:

An Approach to Bridge Inspection Using 3D Laser Scanners and Digital Photographs

_____

Chairperson – Daniel Tran, Ph. D.

Date approved:

Abstract

Bridges are an integral component of infrastructure systems, which play a critical role in the development of the economy, society, and national security. However, bridges have not received adequate care and are deteriorating rapidly. More than 9% of bridges in the United States are structurally deficient and need immediate repairs. A major contributing factor to this deficiency is a lack of adequate and accurate inspection processes. Current methods of bridge inspection and assessment involve a reiterative paper-based process that requires manual data entry and extraction. The inspection team analyzes the critical portions of a bridge, identifies problem severity, documents the damages and concentrates on the cause of the problem. This paper-based process is complex, time-consuming and error-prone. To eliminate human errors attached with surveying and the data collection process, practitioners recently have used automated techniques and advanced equipment to inspect bridge conditions. This research introduces a combination of 3D laser scanning and photographic techniques to determine important attributes of bridge inspection. A terrestrial laser scanner is used to collect point cloud data to create a 3D model of the bridge structure. Three-dimensional geometrical information of bridge structure is extracted from the point cloud 3D model with accuracy level in accordance with national bridge inventory (NBI) specifications. The occurrence of cracks in bridge components is a clear sign of potential damage and must be assessed critically. In order to determine the severity of damage, it is important to compute the width of cracks and compare the data with an allowable limit as specified by NBI or state department of transportation (DOT). In addition, to examine geometrical surveying data, this research proposes a framework to detect cracks in the bridge structure. The framework is verified and validated using a case project. The results of this study

contribute to the construction engineering and management body of knowledge by demonstrating the extraction of geometric data for bridge inspection in accordance with NBI accuracy specifications using a laser scanner. This study also demonstrates an automated technique to assess structural health by detecting cracks in a concrete bridge using digital photographs and computing the width of those cracks.

Dedication

I dedicate this thesis to my parents and family. Their continuous support and prayers have guided me through every difficulty in life and made me who I am today. Love you all.

Acknowledgements

My thesis is an important milestone in my educational and professional career. I gained a lot of useful experience and knowledge that will stay with me forever. I would like to thank and mention every individual that helped me throughout this learning process. First I would like to acknowledge Dr. Tran, my mentor and advisor, who advised me to encourage this topic provided help and guidance throughout.

I would also like to acknowledge Dr. Brian Lines and Professor Michael Panethiere P.E. for always being there for me whenever I needed help or advice.

I would also like to acknowledge the Office of Design and Construction Management at KU for providing me data to validate my findings and also for providing permission for scanning Irving Hill Bridge.

TABLE OF CONTENTS

List of Tables

List of Figures

Chapter 1: Introduction

1.1Introduction

According to the American Society of Civil Engineers (ASCE, 2017), there are over 600,000 bridges in the United States. Most of the bridges that are currently in use were built around 1945 (Meral, 2011). These bridges are approaching the end of design life and starting to show signs of fatigue. When bridges reach their mid-life, they begin to show structural damage. The damage can range from minor cracks to major deformation and deterioration around the edges of deck and piers. Such damages can lead to failure of the bridge. Bridge inspection must be carried out at regular intervals to keep track of damage that occurs over time.

According to the 2017 ASCE report card for American infrastructure, bridges have been given a C+ grade, which is same as the grade they received in 2013. Furthermore, the report card states that as of 2016, over 56,000 bridges are structurally deficient. This accounts for more than 9% of total bridges in the United States. 2013 and 2017 reports by ASCE show no improvement in the bridge condition ratings. Lack of improvement in bridge condition ratings in the past 4 years suggests a passive bridge inspection and repair process.

Geometric data and structural health assessment are important components of the bridge inspection process. The two tasks represent almost all of the field work and data collection required during the inspection process. Any improvement to the methodology of these two tasks will result in the overall improvement of bridge inspection process. As of 2017, geometric data is collected using theodolite and other semi-automatic machines that require multiple surveyors and

occasional closure of traffic lanes. On the other hand, the assessment of bridges' structural health is conducted by an inspector via visual inspection. Both methods are error-prone and time-consuming. This research introduces a combination of 3D laser scanning and photographic techniques to determine important attributes of bridge inspection. A terrestrial laser scanner is used to collect point cloud data to create a 3D model of the bridge structure. Three-dimensional geometrical information of bridge structure is extracted from the point cloud 3D model with accuracy level in accordance with national bridge inventory (NBI) specifications. In addition, this study also demonstrates an automated technique to assess structural health by detecting cracks in a concrete bridge using digital photographs and computing the width of those cracks.

1.2 Motivation

NBI requires state departments of transportation (DOTs) biennial inspection of each bridge to assess any damage to its structure. Bridge inspection provides necessary oversight for continued performance of bridge structure at a desirable level. As discussed in the previous section, most of the nation's bridge are edging towards the end of their design life and are showing signs of deterioration. This requires more accurate and rapid inspection process to maintain the integrity of bridge structures, emphasizing the importance of the accurate and reliable geometric information of the bridges. Geometric data, such as maximum span and minimum vertical clearance, are the main parameters of bridge inspection process. The conventional method of obtaining bridge inspection data is slow and error prone (Meral, 2011). In order to acquire precise data in time efficient manner, automated techniques, such as 3D laser scanner and digital photographs, should be used.

A 3D Terrestrial laser scanner is a relatively new technique that provides the ability to acquire rapid and accurate data for bridge surveying. In recent years, laser scanners have been introduced rapidly into the design and manufacturing industry. Many studies have been conducted to integrate laser scanner technology in civil infrastructure projects. Laser scanners are a reliable technology for geometric data collection. Although laser scanners enable surveyors to acquire the data in shorter time, data accuracy should be investigated. The main objectives of this study are to investigate and evaluate the accuracy of laser scanners for bridge inspection and to determine the reliability of laser scanners data.

In addition to geometric data collection for bridge inspection, there is a need to develop rapid methods for collecting and analyzing data for assessing the health of structural components of bridges. Fatigue can cause cracks in bridge deck and piers which can result in reduced performance. This study employs image-based crack detection to analyze the structural deficiencies of bridge components. The image-based crack detection was analyzed and verified through a computational process coded in MATLAB.

1.3 Research Objectives

As discussed previously, the primary objective of this research is to validate the accuracy of 3D laser scanner data for bridge inspection and assessment. A list of NBI bridge inspection items that require geometric data is used as a reference to assess the accuracy of laser scanner data. NBI provides a desirable level of accuracy for each item on the bridge inspection checklist.

Collected data was compared to the as-built drawings of bridges and errors in each measurement were computed. Computed errors were validated by comparison with NBI requirements.

The second objective of this research is to provide a working proof-of-concept for an image-based crack detection and crack width computational algorithm. Photographs from a high-resolution camera are used to detect the cracks in bridge structure and compute their width.

1.4 Reader's Guide to This Thesis

Chapter 2 provides a background study on a bridge inspection process and historical events that shaped the current NBI regulations. This chapter describes the detailed motivation of this research.

Chapter 3 introduces the terrestrial laser scanning process and crack detection. This chapter provides a detailed overview of automated techniques that are key to this research.

Chapter 4 provides an overall framework of research methodology. Chapter 4 also provides an overview of research equipment and error sources associated with data collection process.

Chapter 5 provides detailed data collection and analysis conducted during the research and also discusses the results obtained.

Chapter 6 summarizes the thesis and discusses the results obtained in Chapter 5. Chapter 6 also provides the findings and lists the lessons learned from this study.

Chapter 7 provides the final conclusion for the thesis and recommendations for future studies.

Chapter 2: Background and Motivation

2.1 Introduction

Bridges are an integral component of infrastructure systems, which play a critical role in the development of the economy, society, and national security. However, bridges have not received adequate care and are deteriorating rapidly. Demands on limited resources, especially competing for roadway priorities for increased capacity and improved riding surfaces, often result in deferred maintenance for bridges. The consequences may lead to bridges deteriorating faster than they are being repaired. Without adequate attention, many bridges require replacement or closure long before they are really obsolete. This problem is impacting safety and discouraging both users and transportation providers (New York State Department of Transportation (NYSDOT), 2008).

According to Federal Highway Administration (FHWA), there are almost 600,000 highway bridges in the United States, (ASCE, 2017). The average life span of these bridges is about 70 years since most of the bridges were built around 1945. As bridges reach half of their life span, damage starts to occur. This can be anything from a small crack or corrosion to deflection or deformation. All these damages can reduce bridge's load carrying capacity. Thus, all bridge members should be inspected periodically (Meral, 2011).

In 2017, the ASCE released the ASCE Report Card for America's infrastructure. This report depicts the current condition and performance of the nation's infrastructure (ASCE, 2017). In this report, the average grade for all infrastructure types was a D+, and the grade given for

bridges specifically was a C+. This grade is the same as given in the 2013 report card. Lack of improvement suggests insufficient inspection and repair activities.

2.2 Background of Bridge Inspection

The practice of bridge inspection has traditionally been a reactive rather than a proactive measure. Responses to disasters have led to the development of bridge inspection and maintenance. Many major collapses resulted from material failures that might have been identified beforehand by periodic inspection and maintenance. This could have prevented the disaster. With each failure, new facts were learned and new standards implemented. In 2008, NYSDOT published a report discussing a short list of some events that have dramatically influenced inspection and maintenance practice.

During the bridge construction boom of the 1950s and 1960s, little emphasis was placed on safety inspection or maintenance of bridges. This changed when the 2235-ft Silver Bridge at Point Pleasant, West Virginia, collapsed into the Ohio River on December 15, 1967, killing 46 drivers and passengers. This tragic accident aroused national concern about bridge safety inspection and maintenance. The United States Congress added a section to the Federal Highway Act of 1968, requiring the Secretary of Transportation to establish national standards for bridge inspection and to develop a program to train inspectors. Thus, in 1971 National Bridge Inspection Standards (NBIS) were created, setting a national policy for inspection frequency, inspector qualifications, reporting formats, and procedures for inspection and rating of bridge conditions. It is noted that during the 1970s, attention was also directed to culverts after several

collapses claimed more lives, although culverts had not originally been included in these new programs.

In 1983, the Mianus River Bridge in Connecticut collapsed after one of its pin-and-hanger assemblies failed, leading to an emerging national emphasis on fatigue- and fracture-critical elements. With the April 1987 collapse of the Schoharie Creek Bridge on the New York State Thruway, new attention also focused on underwater inspection of bridge foundations.

The FHWA bridge inspection program regulations were developed as a result of the Federal-Aid Highway Act of 1968 (sec. 26, Public Law 90-495, 82 Stat. 815, at 829) that required the Secretary of Transportation to establish the NBIS. The primary purpose of the NBIS is to locate and evaluate existing bridge deficiencies to ensure the safety of the traveling public.

The 1968 Federal-Aid Highway Act directed the States to maintain an inventory of Federal-aid highway system bridges. The Federal-Aid Highway Act of 1970 (sec. 204, Public Law 91-605, 84 Stat. 1713, at 1741) limited the NBIS to bridges on the Federal-aid highway system. After the Surface Transportation Assistance Act of 1978 (STAA) (sec. 124, Public Law 95-599, 92 Stat. 2689, at 2702) was passed, NBIS requirements were extended to bridges greater than 20 feet on all public roads. The Surface Transportation and Uniform Relocation Assistance Act of 1987 (STURRA) (sec.125, Public Law 100-17, 101 Stat. 132, at 166) expanded bridge inspection programs to include special inspection procedures for fracture critical members and underwater inspection.

Over the years, varying amounts of federal funds have been spent on bridge projects, depending on the demands of the transportation infrastructure. Figure 2.1 shows fluctuations in federal spending and shows current trends (FHWA, 2012).

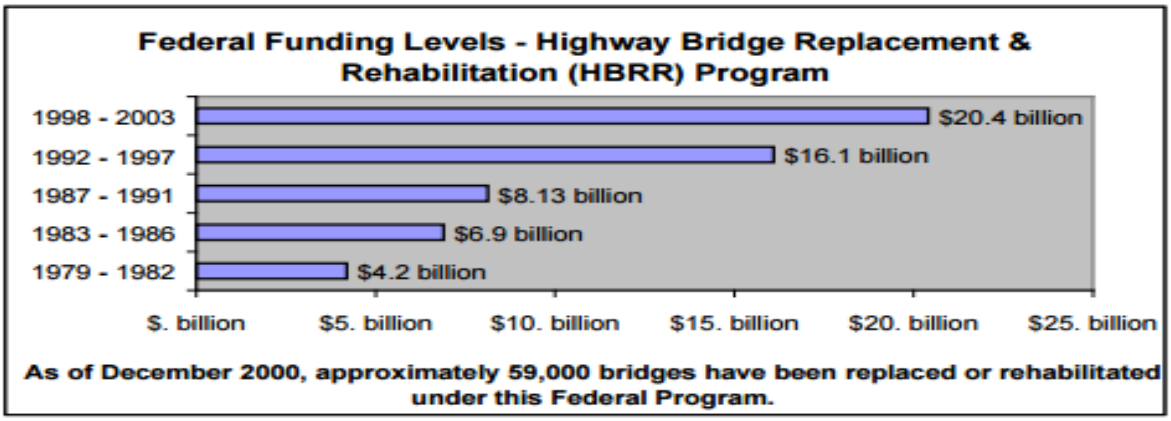

Figure 2.1: Federal Funding levels (FHWA, 2012)

2.3 Process of Bridge Inspection

To understand the bridge inspection process, it is important to understand two key aspects of bridge inspection: (1) types of bridge inspection, and (2) Inspection methodology. Depending upon the circumstances, under which bridge inspection is being conducted, the type of inspection can be determined. NBI Codes of Federal Regulations have issued a list that identifies different types of bridge inspection. After determining types of bridge inspection, appropriate inspection parameters and methodology can be devised. Although the overall process of bridge inspection is similar to each type, special updates can be made to previously determined methodology depending upon the situation.

2.3.1 Types of Bridge Inspection

Federal Codes of Regulations (NBIS, 2004) classifies bridge inspection into several different types depending on the type of damages and circumstances under which inspection is taking place. Aside from regular inspections that take place every 18-24 months on most of U.S. bridges, special events, or environmental disaster can lead to unscheduled inspections. There are five basic types of bridge inspections, including initial inspection, routine inspection, damage inspection, in-depth inspection, and interim inspection. Types and procedure for bridge inspection discussed in this section are based on information provided in Federal Codes of Regulation Title 23 (See references section for details). The following sections discuss these types of inspection in detail.

2.3.1.1 Initial inspection

The Code of Federal Regulations contains the NBIS. The NBIS require inventory information to be entered into the State's database within 90 days after the bridge is placed in service (begins carrying traffic). Before entering the bridge information into state's database, an initial inspection takes place. Initial inspection can also refer to the inspection carried out on an existing bridge to collect information before adding the bridge to state's database. This inspection provides a basis for all future inspections or modifications to a bridge. If the inspection is carried out on an existing bridge, the purpose is to note initial deficiencies which might not have been present at the time of construction.

Initial inspection on a new bridge is required before notifying the district bridge inspection coordinator that the bridge is opened to traffic and available for use by permit vehicles. The opening of a new bridge, particularly an off-system bridge, is a good time to ensure that a copy of the bridge plans is included with the bridge records. Initial inspection helps prepare the initial bridge folder or bridge record that is used as a basis for every inspection that may follow.

2.3.1.2 Routine Inspection

Routine inspections are conducted at an interval of every 24 months' interval for most DOTs (Transportation Research Board, 2007). Routine inspection is the intermediate level inspection consisting of sufficient observations and measurements to determine the physical and functional condition of the bridge. Inspection data is used to identify any developing problems or changes from "inventory" or previously recorded conditions and to ensure that the structure continues to satisfy present service requirements.

The routine inspection must fully satisfy the requirements of the NBIS with respect to inspection frequency, updating of structure inventory and appraisal data and the qualifications of the inspection personnel. These inspections are generally conducted from deck, ground or water levels, and from permanent work platforms and walkways. Special equipment (e.g., under-bridge inspection equipment, rigging, or staging) is used for routine inspection in some circumstances. Special equipment is used where its use provides the only practical means of access to areas of the structure that are being monitored.

The results of a routine inspection are fully documented with appropriate photographs and a written report that includes any recommendations for maintenance or repair and for scheduling of follow-up in-depth inspections (see the section below for more details). Load capacity evaluations are provided to the extent that changed structural conditions would affect any previously recorded ratings.

2.3.1.3 Damage Inspections

Damage inspection is conducted in response to a disaster or weather anomaly. This inspection is also referred to as event-driven inspection. This is an unscheduled inspection to assess structural damage resulting from environmental or man-inflicted causes. The scope of inspection must be sufficient to determine whether there is a need for an emergency load restrictions or closure of the bridge to traffic and to assess the level of effort necessary to affect a repair. The amount of effort expended on this type of inspection varies significantly depending upon the extent of the damage (Transportation Research Board, 2007). If major damage has occurred, inspectors must evaluate fractured members, section loss, make measurements for misalignment of members and check for any loss of foundation support. A capability to make on-site calculations to established emergency load restrictions may be necessary. This inspection may be followed up by a timely in-depth inspection (explained in next section) to document more fully the extent of damage and to compute the urgency and magnitude of repairs. Damage inspection requires follow-up procedures such as proper documentation, verification of field measurements and calculations and perhaps a more refined analysis to establish or adjust interim load restrictions. A particular awareness of the potential for litigation must be exercised in the documentation of damage inspections.

2.3.1.4 In-Depth Inspections

An in-depth inspection is a close-up, hands-on inspection of one or more members above or below the water level to detect any deficiencies not readily visible using routine inspection procedures. Traffic control and special equipment (e.g., under-bridge inspection equipment, staging, and workboats) may be required to obtain access. This type of inspection needs personnel with special skills such as divers and riggers, depending on elements that need to be inspected. In-depth inspection often requires nondestructive tests and other physical and chemical tests in order to fully ascertain the existence and the extent of any deficiency.

The inspection includes a load rating to assess the residual capacity of the member or members, depending on the extent of the deterioration or damage. This type of inspection can be scheduled supplement to a routine inspection, though generally at a longer interval, or it may be a follow-up for damage or inventory inspections.

On small bridges, the in-depth inspection, if warranted, include all critical elements of the structure. But for large and complex structures, in-depth inspections may be scheduled separately for defined segments of the bridge or for designated groups of elements, connections or details that can be efficiently addressed by the same or similar inspection techniques. If the in-depth inspection is performed on a specific bridge segment, each segment or section of a bridge is recorded separately. Each section or segment is also assigned a frequency for re-inspection. It is necessary to completely and carefully document the procedures and the findings of the in-depth inspection. In-depth inspections are treated more carefully than routine and initial inspections.

2.3.1.4 Interim Inspections

This is an inspection scheduled at the discretion of the individual that is in charge of bridge inspection activities. Interim inspection is used to monitor a particular known or suspected deficiency (e.g., foundation settlement or scour, member condition, the public's use of a load-posted bridge, etc.). Interim inspection can be performed by any qualified person familiar with the bridge and who is available to accommodate the assigned frequency of investigation. The individual performing interim inspection must be carefully instructed regarding the nature of the known deficiency and its functional relationship to satisfactory bridge performance. Inspectors must be provided with the guidelines and procedures on what to observe and measure. Further, the inspector should follow a timely process to interpret the field results.

2.3.2 Bridge Inspection Methodology

The bridge inspection process being followed by DOTs throughout the United States follow a similar pattern. To conduct the literature review for our research, we focused on the bridge inspection process outlined by Florida DOT in 2008. The inspector often starts with reviewing previous bridge inspection reports to identify the defects found in the past before planning the current inspection (Florida DOT, 2008). The inspector then coordinates traffic control plans to avoid any hurdles during data collection. A complete assessment of survey equipment is also done before starting the data collection process.

At bridge site, the inspector observes the bridge to identify major problems like the smoothness of bridge profile. Bridge inspector observes any irregularities in the structure and relies on

his/her experience to analyze its extent and severity. The inspector concentrates on discovering the cause and determining the extent of the problem. Depending on the exact nature of the problem, emergency repair or immediate closure of the bridge may be required. This process is typically conducted along with the previous inspection report to determine if the defects previously identified have been repaired or have increased in size and severity.

Bridge inspectors employ a systematic inspection process to ensure that the complete bridge is inspected. Order of this system might differ with the type of bridges being inspected. Different parts of bridges are inspected for specific defects. Details of this system are shown in Figure 2.2.

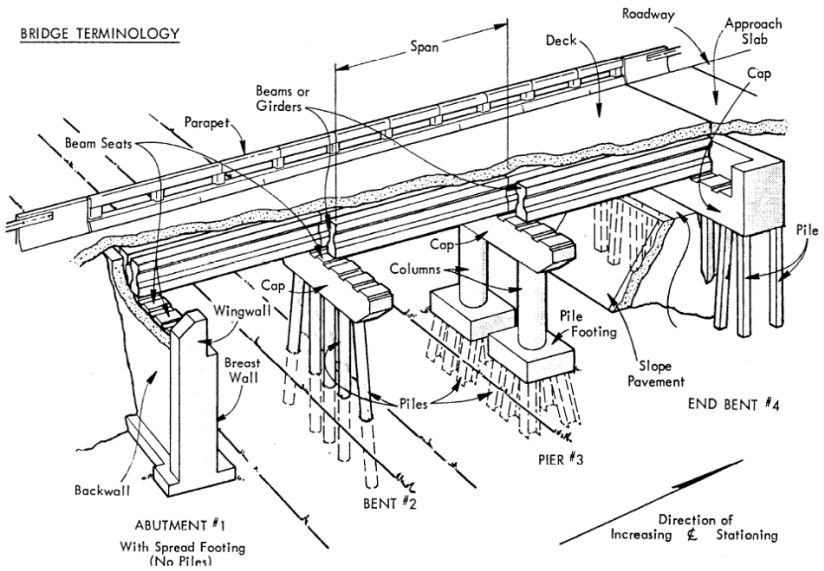

Figure 2.2: Bridge Terminology (Source: Florida DOT, 2008)

Bridge inspection includes careful examination of each component of the bridge structure. The inspection procedure for each component of the bridge shown in Figure 2.2 is discussed in the

next section. The detailed methodology explained below is based on Florida DOT's bridge inspection manual and American Association of State Highway and Transportation Officials (AASHTO)'s bridge inspection Manual (AASHTO 2011). See references section for details to look up both studies.

Bridge Deck

The inspection of the bridge deck involves examining potholes, cracking, excessive wear and sounded for hollow areas. Joints are examined for evidence of seepage, loose armor angles. The purpose of inspecting the joints to understand if they are properly functioning to allow expansion and contraction due to temperature change.

Superstructure

The superstructure supports the deck and generally consists of (1) beams or girders that may be constructed of timber, concrete or steel, and (2) the bearings that connect the superstructure to the substructure. Timber members are inspected for wood rot, crushing, splitting and cracking. Concrete members are inspected for cracking, spalling and hollow areas. Steel members are inspected for paint peeling, corrosion, and cracking. The bearings serve to transmit loads from the superstructure to the substructure and allow the movement of bridges that occur due to changes in temperature. The bearings are inspected for excessive deformation and evidence whether they are functioning properly.

Substructure

The substructure supports the superstructure and transmits loads from the superstructure to the ground. The substructure generally consists of pier caps, columns, and piles. The substructure may be constructed of timber, concrete or steel. Similar to the superstructure, timber members are inspected for wood rot, crushing, splitting, and cracking. Concrete members are inspected for cracking, spalling, and hollow areas. Steel members are inspected for paint peeling, corrosion, and cracking. In addition, the substructure is inspected for evidence of settlement or scour.

After the detailed inspection of all the bridge elements, the inspector will take actions. According to the result of the inspection process, the inspector may suggest immediate closure or emergency repairs on affected sections. The inspectors will recommend a repair be performed quickly for a situation that, if not addressed in a timely manner, could endanger the public. The inspectors will recommend routine repairs or maintenance to correct defects that if not repaired properly could increase in size and severity and shorten the service life of the bridge.

Florida DOT 2008 (see references section for details) states that the bridge inspectors are required to document their findings in the bridge inspection report, which contains the following:

- Inventory data such as location, bridge name, roadway, facility crossed, geometric and others;
- Verbal descriptions of the inspectors' findings including size and severity of defects found;
- Pictures and sketches of portions of the bridge to clarify the verbal descriptions;
- Inspector recommendations;

- Evaluation of work performed on the bridge since the last inspection;
- Names of the inspectors, report reviewer, and responsible professional engineer;
- Date and type of inspection performed;
- Numerical ratings of various bridge components;
- Values of the Sufficiency Rating and Health Index;

Figure 2.3 shows a workflow of current bridge inspection process. Figure 2.3 summarizes the inspection process that is discussed in the section above. Bridge inspection process starts by a visit to the site. During the visit, data is collected on bridge geometry and conditions. NBI has provided with a bridge inspection checklist. Every item on this list must be checked off for a thorough inspection. NBI has also provided with a condition rating index that is used to rate the bridge component. The method of data representation and documentation of inspection results varies among different DOTs. Figure 2.3 represents the inspection workflow of Oregon DOT.

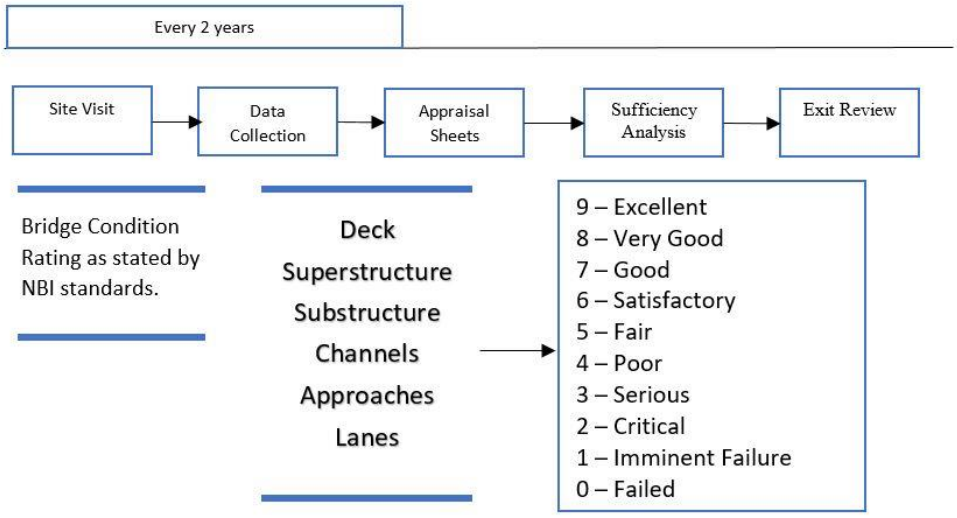

Figure 2.3: Workflow of bridge inspection process (Based on Oregon DOT's bridge inspection workflow)

2.4 Summary

The current bridge inspection practices being used by most states are a manual, paper-based, and time-consuming process. The nature of the current inspection process makes it error-prone and time-consuming. It is time to include automated techniques into the bridge inspection process. The inclusion of techniques such as Terrestrial Laser Scanner will provide a digital database for bridge inventory with more accurate results. State DOTs are employing new automated systems to make the bridge inspection process more accurate and efficient.

Chapter 3: Literature Review

3.1 Introduction

This chapter of the thesis discusses the literature review section for automation in the bridge inspection process. This chapter also reviews the literature on laser scanning technology and use of laser scanners in various industries. The final section of this chapter focuses on crack detection techniques in the bridge structure.

3.2 Integration of New Techniques in Bridge Inspection

Bridge condition inspection data provides rich and critical information for assessing structural condition. According to a revision to NBIS in 1988, the FHWA requires all state DOTs to perform biennial inspection for each bridge to examine and document its condition. In order to evaluate the current status of bridge's aging, deteriorating, and damaged structures, it is vital to accurately assess their present conditions. It is possible to capture the in-situ condition of structures by using laser scanners that create dense three-dimensional point clouds. Laser scanning technology is continuously improving, with commonly available scanners now capturing over 1,000,000 texture-mapped points per second with an accuracy of ~2 mm (Guldur, 2014). However, automatically extracting meaningful information from point clouds remains a challenge, and the current state-of-the-art requires significant user interaction.

In the United States, the NBI program requires bridge inspectors to inspect more than 600,000 bridges at least once every two years. NBI has a list of 116 data items that are used to inspect

bridges. Out of those 116, 16 are related to geometric data acquisition (Tang et al. 2007). The implication of automated data collection techniques like 3D Laser Scanner directly improves the accuracy of these data items.

Table 3.1: Geometric Data Items in NBI and their Accuracy Requirements

Item Name	Precision Requirement
Skew	1 degree
Minimum Navigational Vertical Clearance	3.93 inches
Structure Length	3.93 inches
Maximum Span Length	3.93 inches
Curb or Side Walk Width	3.93 inches
Bridge Roadway Width	3.93 inches
Deck With, out to out	3.93 inches
Approach Road Width	3.93 inches
Minimum Lateral Under Clearance on Right	3.93 inches
Minimum Lateral Under Clearance on Left	3.93 inches
Inventory Total Horizontal Clearance	3.93 inches
Navigation Vertical Clearance	3.93 inches
Navigational Horizontal Clearance	3.93 inches
Inventory Route Minimum Vertical Clearance	0.393 inches
Minimum Vertical Under Clearance	0.393 inches
Minimum Vertical Clearance over Bridge Roadway	0.393 inches

Table 1 shows the NBI requirements for a certain degree of precision when collecting geometric data. The accuracy of data is crucial in producing a reliable bridge inspection report. In spite of these facts, current bridge geometric data collection methods are time-consuming and error-prone because they rely on manual data collection methods (Sanford et al. 1999).

Lack of automation has made initial steps of construction, such as surveying and progress data collection, difficult and time-consuming mostly because of relying on 2D data sets. This research explored ways to collect and analyze construction data in, a more interactive and efficient, 3D medium. To address this issue, the proposed research concentrates on investigating the possible applications of 3D laser scanning in the field of data collection, surveying, bridge inspection, as-built modeling and other construction engineering and management problems.

3.3 Types of 3D Laser Scanner

Depending on the host, laser scanners can be classified as either hand-held, aerial or terrestrial laser scanner. Each type can serve a unique need and help capture data more effectively. Hand-held scanners are small and easy to carry, they are commonly used in the business world to scan bar codes and product detail tags. More powerful hand-held scanners have applications in mining, concept prototyping and in labs to scan irregular objects with great detail. These scanners provide great mobility and ease while operating. Hand-held scanners use an internal coordinate system to map a surface.

Figure 3.1: Hand-held laser scanner (makepartsfast.com)

On the other hand, aerial laser scanners are mounted on a quadcopter or bottom of the airplane. The working concept is very similar to that of photogrammetry and is useful to map a terrain with pinpoint precision.

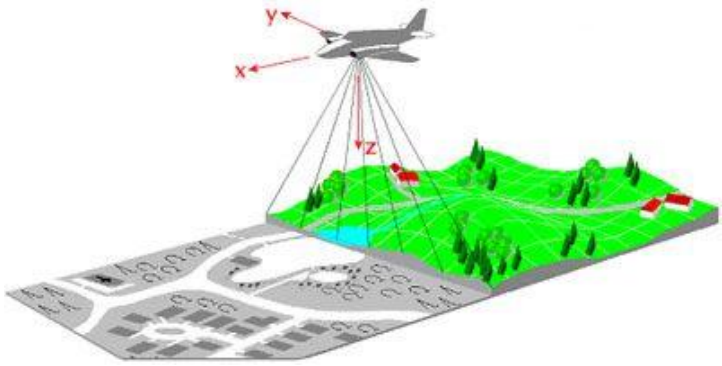

Figure 3.2: Aerial laser scanning operation (Source: projects.unwell.com.au)

Terrestrial laser scanners are most commonly used in surveying for construction projects. These scanners are equipped with a laser beam, a global positioning system (GPS) and a camera and

are mounted on a tripod stand while in use. Terrestrial laser scanners use the concept of triangulation and time-of-flight method to map its surroundings and store data in a point cloud format. For this research, a Trimble TX5 terrestrial laser scanner was used.

Figure 3.3: Terrestrial laser scanner (Source: google images)

3.4 Laser Scanner Operating Principle

The 3D laser scanner is an advanced data acquisition system which enables users to gather spatial data with precision and speed. 3D laser scanner scans real world objects around it to gather data on their shape, appearance, and relative position and store it in point cloud format, which is available, digitally, to users for 3D modeling. It has become one of the most accurate and fastest data acquisition techniques compared to existing surveying techniques, such as a theodolite, total station (Chen et al. 2005). The application of laser scanners can be found in

multiple domains, such as archeology, architecture, aviation, meteorology, defense, surveying and construction (Lichti et al. 2006).

The 3D laser scanner technology operates on a similar principal as that of Light Detection and Ranging (LIDAR). LIDAR is an optical remote sensing technique that uses ultraviolet, visible or near infrared light to image objects. It sends a beam of light to the target and detects the reflecting ray that bounces back off the object surface and calculates the distance on the basis of time between emission and detection of two rays (emitted and reflected). In a laser scanner, a laser beam is used to measure the distance of objects. Since laser beams have a shorter wavelength (10 micrometers), it allows to detect a smaller object and measure the relative distance. Every point that laser scanner detects is stored in a point cloud data. When a scan is complete, these points together represents the shape of the actual object.

3.5 Applications of 3D Laser Scanner in Modern World

Aside from construction and surveying, a 3D laser scanner has a diverse range of applications in different industries and fields. Different researchers have found a 3D laser scanner to be an extremely useful tool for collecting data and reconstructing models. 3D object scanning allows enhancing the design process, speeds up and reduces data collection errors, saves time and money, and thus makes it an attractive alternative to traditional data collection techniques. Some applications of a 3D laser scanner in modern world are discussed here

3D laser scanners are being extensively utilized in industrial design. Automobile design companies are rapidly adapting laser scanner technology for design processing.

There have been many research projects undertaken via the scanning of historical sites and artifacts both for documentation and analysis purposes. The combined use of 3D scanning and 3D printing technologies allows the replication of real objects without the use of traditional plaster casting techniques. This technique helps to recreate delicate heritage object that is too delicate for excessive examination.

3D scanners are used by the entertainment industry to create digital 3D models for movies, video games, and leisure purposes. They are heavily utilized in virtual cinematography. In cases where a real-world equivalent of a model exists, it is much faster to scan the real-world object than to manually create a model using 3D modeling software. It also provides the ability to frequently scan objects, physical feature, and models rather than individually modeling them using computer software.

3D laser scanning is also being used by the FBI and other law enforcement agencies. 3D Models are used for on-site documentation of

- Crime scenes
- Bullet trajectory
- Accident reconstruction
- Bombings
- Plane crashes, and more

Reverse engineering of a mechanical component requires a precise digital model of the objects to be reproduced. Rather than a set of points a precise digital model can be represented by a polygon mesh, a set of flat or curved surfaces, or ideally for mechanical components, and a CAD solid model. A 3D scanner can be used to digitize free-form or gradually changing shaped

components as well as prismatic geometries whereas a coordinate measuring machine is usually used only to determine simple dimensions of a highly prismatic model. These data points are then processed to create a usable digital model, usually using specialized reverse engineering software (Thilmany, 2012).

3.6 Applications of 3D Laser Scanners

Laser scanning has, in recent years, rapidly established a significant and diverse range of applications in areas including engineering, construction, architecture and heritage (Cignoni and Scopigno, 2008). There are numerous studies in the literature highlighting recent and potential applications for 3D laser scanning in these fields and offering comparisons with alternative forms of data acquisition.

A 3D scanner is a relatively new device that uses laser line beams to collect spatial data points, spatial relationships, and dimensions of the object. It is a digital data collection technology. The scanner outputs a point cloud image, which accurately replicates the scanned objects. Depending on the type and make of the scanner, objects can be scanned from up to several hundred meters, and data points can be collected to the accuracy of less than 5mm at speeds from several thousand to several hundred thousand points per second (Gurjar and Prakash, 2017). The overall speed depends on the desired density of the point cloud. When an object is too large to be captured in a single scan, multiple scans from different lines of sight can be linked together to complete the point cloud image. Once the 3D point cloud is generated, the data can be exported to many common CAD, modeling and BIM programs to generate 2D CAD drawings or a 3D model (Fallon, 2012).

Laser scanning is an established technology to acquire rapid spatial data in Architecture, Engineering, and Construction (AEC) sector with a wide range of applications (Alizadehsalehi et al. 2015). An understanding of the wide variation of technical requirements and considerations associated with these applications is critical to making decisions about laser-scanning implementations on projects (Randall 2011).

3D models have application in a wide range of construction projects including building, bridge investigation, and repairs, road survey, and modeling etc. In the AEC domain, semantically rich 3D information models are increasingly used throughout a facility's life cycle for diverse applications, such as planning renovations, space usage planning, and managing building maintenance (Xiong et al. 2013).

Progress reporting is an essential management function for successful delivery of a construction project (El-Omari and Moselhi 2008). An accurate and fast method to collect data on a construction site is 3D scanning, where the construction site is scanned and different times to generate data. This data can then be used to estimate the quantities of work performed within the time interval between two scans and thus help keep track of progress.

Accurate and rapid assessment of the as-built status on any construction site provides the opportunity to understand the current performance of a project easily and quickly (Golparvar-Fard et al. 2011). This assessment is crucial to project success. Manual Data collection is one of the most labor-intensive tasks when monitoring a project’s progress (Cho et al. 2002). In some cases, a field engineer spends half of every work day in collecting and recording this data and comparing it with his superintendent.

Rietdorf et al. (2003) made the first report on terrestrial laser scanner calibration. He presented point-on-plane condition models and create a self-calibration of TLS in terms of vertical index error, horizontal collimation error, and eccentricity. They mentioned about their use of planar targets rather than point targets and some aspects of their network design.

Gielsdorf et al. (2004) proposed error models and a calibration method using planar targets for the low-cost 3D laser scanner they built in order to increase the data accuracy. The parameters of this research are trunnion axis error, vertical index error, horizontal collimation error, additive rangefinder constant and eccentricity. The determination of calibration parameters is based on a calibration field (Meral, 2011).

3.7 Cracking in Concrete Bridges

3.7.1 Background

NBI bridge inspection manual includes cracks as a major criterion of determining bridge health. Item 58, 59, 60 and 62 in NBI bridge inspection manual provides a detailed index of bridge component condition rating and criteria of determining it. Cracks in the bridge deck, superstructure, substructure, and culverts must be evaluated and monitored during the biennial bridge inspection to better assess bridge health. Different factors can play a role in the cracking of bridge structures e.g. design parameters, use of faulty materials and construction parameters.

It is well-known that concrete has relatively low tensile strength, and this characteristic is one of the important causes of cracking. In its early age, concrete cracking occurs due to the restraint of the concrete. The volumetric movement of the concrete is prevented by restraint, which is

produced by either internal or external sources (Ganapuram et al. 2012). Internal sources of restraint are steel reinforcement in the bridge deck and aggregates in the concrete (Brown et al., 2001). External sources of restraint are produced by the superstructure, friction between the bridge deck and supporting girders, and the sub-base (Brown et al., 2001). Because the bridge deck and superstructure act compositely, the bridge deck undergoes large amounts of restraint because no relative displacement can occur. Therefore, concrete cracks become visible when the tensile strength of the concrete is exceeded by the tensile stresses produced by restraint. These tensile stresses ultimately turn into cracks that can adversely affect the performance of concrete.

A major cause for cracking in concrete bridges is the nature of concrete. Concrete tends to shrink at an early age. In order to counter this problem, it is important to prevent evaporation of water from the concrete surface. This is achieved by fogging or curing immediately after concrete placement. Lwin and Russell (2006) suggest that the most effective strategies to control cracking are fogging during placement of the fresh concrete and adequate curing during and soon after the hardening of concrete. Fogging gives concrete an adequate amount of water during placement and curing prevents surface evaporation of water after the concrete has hardened.

3.7.2 Previous Work on Crack Detection

Condition assessment of bridge decks plays a vital role in maintaining the structural health and reliability of concrete bridges. Early detection of small cracks on bridge decks is an important maintenance task (Prasanna et al. 2014). More than 100,000 bridges across the United States have exhibited early age bridge deck cracking (La et al. 2013).

Automated and accurate condition assessment that requires minimal lane closure is highly desirable for fast large-area evaluation. Robotic bridge scanning is revolutionizing the process of bridge inspection. Previously, many automated crack detection algorithms for bridge decks emphasize high-contrast visually distinct cracks. Standard image processing methods, including edge following, image thresholding, and morphology operations, are applicable for these cracks. Numerous successful approaches have been demonstrated with high-contrast, low-clutter crack regions as described by (Nishikawa et al. 2012; Zhu et al. 2011; Yamaguchi et al. 2010). Image processing has been utilized to detect cracks in concrete surfaces for diagnosis. Lee et al. (2013) proposed a bridge inspection system to detect cracks in bridge surfaces automatically or under the supervised manipulation of remote controllers. However, the crack images from the real concrete bridge decks are often immersed in significant visual clutter. In this research, a new approach is put forward that to remove noise clutter from crack images and compute crack width by using MATLAB codes.

3.8 Summary

This chapter provides an overview of the laser scanning technology and its uses. This chapter also discusses the different types of the laser scanner and different industries that implementing laser scanning techniques to gain an advantage. The power of laser scanning technology lies in a high data collection rate and a high accuracy. Speed and accuracy are two crucial aspects of any surveying process and 3D laser scanner provides a remarkable advantage in this regard. However, the implication of 3D laser scanning in bridge inspection has its challenges and limitations. This chapter also discusses the previous studies on implications of laser scanning in

the construction industry. Finally, chapter 3 concludes with a brief discussion of crack detection techniques and previous approaches on image-based crack detection methods.

Chapter 4: Research Methodology and Equipment

4.1 Introduction

This chapter discusses the research methodology for this thesis. The chapter starts by discussing the theoretical point of departure for research thesis. This chapter also states the research questions that are investigated in chapter 5. This chapter introduces the research framework and describes the details of the work done in each step of the proposed research framework. A detailed explanation of individual research task is provided. It also provides an overview of data analysis techniques used for this research and different software used to perform those analyses. This chapter also discusses the research equipment. The last section of this chapter discusses different errors associated with laser scanner data.

4.2 Theoretical Point of Departure

The need for this research arises from the fact that the current bridge inspection process is insufficient in dealing with the declining condition of bridges throughout the country. There is an immense need to utilize automated techniques for data collection and analysis while inspecting bridges. The idea of using terrestrial laser scanners and image-based techniques to perform vital bridge inspection tasks has been around for several years but it is still far from becoming a norm in state DOTs bridge inspection process. This research is another step in proving the reliability and workability of automated techniques for bridge inspection by leveraging the speed and accuracy of 3D laser scanner to collect geometrical data. This research thesis investigates the

accuracy of a laser scanner for bridge geometrical data collection against the accuracy limit specified by NBI. Also, this thesis introduces an image-based technique to detect cracks in concrete bridge structures and compute the width of cracks.

4.3 Research Questions

To investigate the research objectives mentioned in Chapter 1 and further extending the point of departure discussed in previous section, this research aimed at investigating following research questions

- How accurate is geometrical data collected using a 3D scanner for bridge inspection? Is that accuracy level in accordance with NBI specifications?How can the image-based crack detection process be used for bridge health determination?

4.4 Research Methodology

The first objective of this research will be the assessment of 3D laser scanning applications in Bridge Inspection and test the accuracy of laser scanner data. The second research objective is a proof-of-concept study to detect cracks in bridge structure using two-dimensional photographs and compute the width of cracks. Figure 4.1 gives an illustrative guide to the research methodology that is implemented in this thesis.

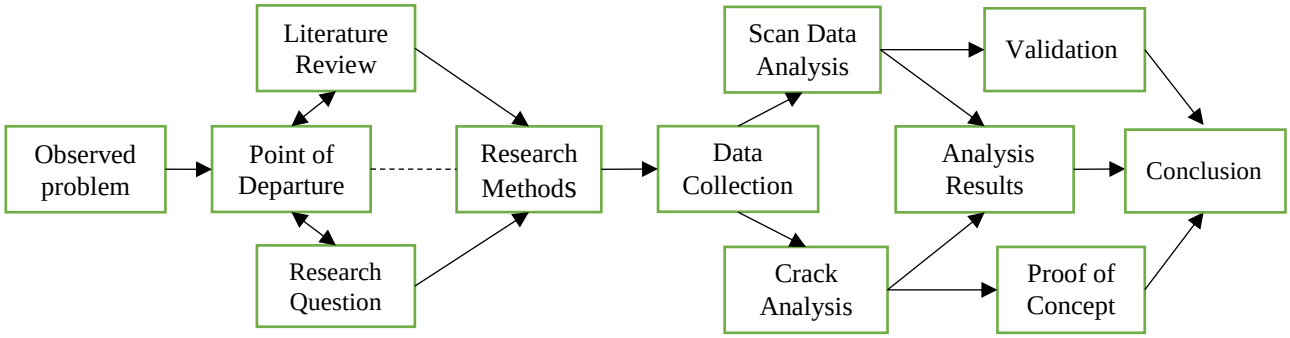

Figure 4.1: Proposed research methodology

The research framework can be divided into 4 major sections: literature review, data collection, data analysis, and data validation.

4.4.1 Literature Review

In light of the observed problem, as discussed in Chapter 1 and research questions stated in the previous section, research was started by performing a detailed literature review on past researches and current implementations of laser scanning in Bridge Inspection. The author gathered all the relevant information from research journals and industry resources to assess the current status of laser scanning applications. This helped to better understand the research potential and also give an overview of current implications of laser technology.

4.4.2 Data Collection

This task will contain the process of data collection using Trimble TX5 laser scanner to make 3D representation models of an existing bridge structure to better understand and visualize the structure. The proposed methodology will leverage high 3D data collection rate of laser scanners for geometric data collection, data process, and data interpretation. The second step of data collection task is to photograph bridge components from various angles.

The Irving Hill Bridge near Daisy Hill in the city of Lawrence, KS is identified to be the most suitable site for data collection. This site is on KU campus and is easily accessible from both sides of Iowa street. Drawings for the bridge are available at KU's Design & Construction Management office. As-built drawings for the bridge were acquired by submitting a formal request to Design & Construction Management office. These drawing will be used to validate point cloud data collected using a 3D laser scanner.

4.4.3 Data Analysis

This task involves the complete analysis and evaluation of proposed model. RealWorks and Autodesk RECAP 360 software will be used to extract geometric data from point cloud 3D model. Geometric data for 15 NBI items will be extracted from laser scanner data. Similar geometric data will also be extracted from drawings acquired from Design & Management Office. Data from as-built drawings will be used to validate the laser scanner data. NBI has provided desirable error ratio for each item. Comparison of data will show the accuracy level of laser scanner data. This process will help visualize the actual application of proposed research

model and assess its performance. The author will also analyze photos taken in the previous step and utilize MATLAB codes to detect cracks in the bridge structure.

4.4.4 Data Validation

After the extraction of geometric information of bridge from laser scanner data, values will be compared with construction drawings. This task will validate the accuracy of gathered data. The error in each geometric measurement will be computed and compared to allow NBI error range discussed in Chapter 3.

4.5 Research Equipment

Equipment used for research is a Trimble TX5 3D laser scanner. TX5 is available with Dr. Tran in construction management laboratory at University of Kansas (KU). The Trimble TX5 high-speed 3D laser0 scanner is able to measure at speeds of up to 976,000 pts/sec and up to a range of 120 m.

TX5 also includes an integrated color camera featuring an automatic 70 megapixels' parallax-free color overlay. It has a size of only 240 mm x 200 mm x 100mm (9.5 in x 8 in x 4 in) and weight of just 5.0 kg (11 lb), it is easy to move and set up in complex environments. The scanner also comes with a lithium-ion battery that provides up to five hours of battery life and can be charged during operation. The option to operate via WLAN to remotely start, stop, view or download scans from a distance is also available.

Figure 4.2: Trimble TX5

4.6 Data Accuracy for Laser Scanner

Due to the rapid increase in the use of laser scanner, it is important to connect each type of laser scanner with appropriate applications. Each manufacturer publishes a statement of requirements which must be satisfied for the advantages of their devices to be differentiated. However, these statements cannot be solely reliable since the accuracy differs among each device and its influences by individual calibration. Research has been conducted to analyze the sources of error in terrestrial laser scanning.

The accuracy of laser scanners can be observed by monitoring different activities where laser scanner is being used. If the models of irregular surfaces and point clouds are affected by point cloud noise or some other effects, the accuracy of the data cannot satisfy the needs.

Equipment used for this research is a terrestrial laser scanner. By looking into previous research conducted by different institutes, the error sources associated with equipment at hand can be concluded. Instrumental errors, errors related to the form and nature of the scanned object, errors resulting from the environment in which the scan was performed, and methodological errors are the four error sources. These error sources can decrease data integrity of point cloud data.

4.6.1 Instrumental Errors

Instrumental errors can be separated into two sections, systematic and random error. Random Errors influence the precision of measurements such as distance and angles in the case of instruments which is the time of flight principle. Systematic errors can be created by non-linearity of the time and temperature measuring system, which can affect the electronic distance measurements.

4.6.1.1 Laser Beam Width

Laser beam width is one of the most important parameters of a scanner which can significantly affect cloud resolution and positional uncertainty. As mentioned before, laser beam size increases respectively with the distance traveled.

Laser beam width enlargement is linear for long distances so divergence is indicated in terms of initial diameter. The divergence of the laser beam simply has an effect on the distance and angle measurements. The location of the observation is along the centerline of the laser beam.

4.6.1.2 Boundary Effects

Boundary effects are can influence the data accuracy. When the laser beam hits a boundary of a surface, it is divided into two parts. Since the same beam hits two different surfaces, a part of the beam will be reflected when the other part will be reflected from a neighboring surface. So, it causes noise at the point cloud and therefore affects the accuracy.

4.6.1.3 Angular Accuracy

A small rotating device is assembled into the laser scanners to deflect the laser beam in a certain direction, such as mirrors or prisms. The rotation of the device causes small angular differences; these differences depend on the distance from the device to the investigated object. These small rotations may cause considerable errors in the coordinates of the points. The greatest factors that impact the angular accuracy are positioning inaccuracies of the rotating instrument and the precision of angular calculation apparatus.

Depending on previous research, effects of these errors can be detectable. Calculating acute horizontal angles and the spatial distance between objects, placed an equal distance from the scanner can assist in detecting the influence of these errors.

4.6.1.4 Axis Errors

Another error often encountered during laser scanning is axis inaccuracy. Laser scanner calibration development yields a geometric model which forces to consider the vertical,

horizontal and collimation axes. The vertical axis, which is also called the principal axis allows the system to move the laser beam horizontally. This is the rotation axis of the scanning unit depending on the type of the scanner. The horizontal axis is described by the rotation axis of the deflecting prisms or mirrors. The collimation axis is the axis of the scanning mirror and the center of the laser spot reflected from the scanned object. These axes are not completely calibrated and accordingly still have the possibility to match with the influence of the errors gained by classical measurement instruments.

4.6.2 Error Due to Nature of Scanned Surface

Laser scanners are assumed to measure the laser beam reflections from the surface of an object. There are some valuable physical laws of reflection and optical features of materials of the inquired object. Depending on the surface, a laser beam can reflect in many directions.

Dark surfaces can absorb a laser beam which causes a weak signal. Therefore, the accuracy of the point gained by the laser beam will be influenced by noise. The surfaces which have high reflection such as white surfaces yield strong signals. Nevertheless, if the surface of the object is a shiny surface, it is difficult to record. The laser beam is totally reflected in a mirroring direction and will hit another surface. When the laser beam is scattered on an irregular surface, the deflection results will cause speckle noise. Reflectance properties of different surfaces can influence the accuracy of point determination. The color of a surface is another factor, which can cause a systematic range difference between two measured values of the same point distance.

4.6.3 Error Due to Environmental Factors

4.6.3.1 Temperature

Temperature is an important parameter which can affect the precision of laser scanning data. Equipment temperature may be higher than the surrounding area due to internal heating of the components and sunlight. This condition can easily merge to distortion of the scan data. Beside this, another important factor which can distort the scan data is the surface temperature. If the scanning surface is hot, due to high temperature, the radiation on the scanned surface will reduce the signal-to-noise ratio during the deflection and can affect the accuracy of the distance measurement.

4.6.3.2 Distortions From Motion

The entire scanning process has a rate of 1 to 3 hours depending on scanning conditions. During this process, the scanner is very sensitive to vibration. Therefore, the scanned object and laser scanner must be fixed and stable. It is a requirement to mount the scanner on a stiff platform in order to avoid the vibration.

4.7 Summary

Chapter 4 provided the theoretical point of departure for the research thesis. Also, this chapter provided the research question that will be investigated during the course of this research. Chapter 4 also provided an overview of research framework that is utilized in this research. The proposed research will feature 4 major section, literature review, data collection, data analysis

and data validation. The Trimble TX5 laser scanner is used for point cloud data collection. Data accuracy of laser scanner can be influenced by various external factors including incident angle, environmental factors, and nature of object surface.

Chapter 5: Data Collection and Analysis

5.1 Introduction

This section of the thesis discusses the data collection and data analysis part of research. The research framework proposed in Chapter 4 was implemented on a case study to depict the workings of proposed research. This section of the thesis is divided into two parts. The first part of this chapter focusses on data collection using a terrestrial laser scanner. Trimble TX5 laser scanner was used to collect point cloud data for Irving Hill bridge in Lawrence, KS. Point cloud data was used to create a 3D model of the bridge structure and geometric data was extracted from the 3D model and validated against the geometric measurements from construction drawings. The second part discusses the data collection and analysis for image-based crack detection, and crack width computation. 2D photographs were captured using the high-resolution camera. MATLAB coding was used to detect the cracks and compute the width of those cracks to assess the structural health of bridge.

5.2 Scanning

5.2.1 Bridge Information

Irving Hill Bridge (Figure 5.1) near Daisy Hill in the city of Lawrence was identified to be a suitable site for data collection. This site is on KU campus and is easily accessible from both sides of U.S. route 59. As-built plans for the bridge are available at KU Design & Construction

Management office. As-built drawings for the bridge were acquired by submitting a formal request to Design & Construction Management office. These drawings were used to validate point cloud data collected using a 3D laser scanner.

Figure 5.1: Irving hill bridge

5.2.2 Fieldwork

The first step of preparation for the scanning process is to decide the location of scans. Due to a time-consuming set-up process, it is important to choose an area that satisfies all of the needs of the experiment. The scanning points should not have any obstructions in line of sight, they should scan the targets directly and the scanner should be positioned where it maximizes the desired scan area. The set ups on the scanning points should not block any progress during the scanning session such as traffic or any other experiments. Laser scanner positioning should be determined to achieve the lowest incidence angle. The number of points on each point cloud can be assigned in scanner settings. Depending on the needs, high-resolution scans can be obtained. However, high-resolution scans can take a lot of time, which is why a moderate resolution was

applied. In order to eliminate less accurate points, only those points were used that lie within 15 meters of scanner location. Prior to the scanning process, following items were accounted

- Trimble TX5 laser scanner.
- Tripod stand.
- Charged batteries.
- SD memory card.

After careful observation of bridge site, ten scan locations were identified underneath the bridge to fully capture all geometric features of above ground substructure and bottom of the superstructure (Group 1). Another two scan locations were identified in order to collect geometric data of superstructure and overlying pavement from the west side of the bridge (Group 2). Due to the vegetation on the sides of the bridge and steep slope, it was difficult to patch the two group of scans. In order to overcome this problem, four more scans (Group 3) were taken on the west side of U.S. route 59. Each scan took 15 minutes to complete. Figure 5.2 shows the positioning of each scan group.

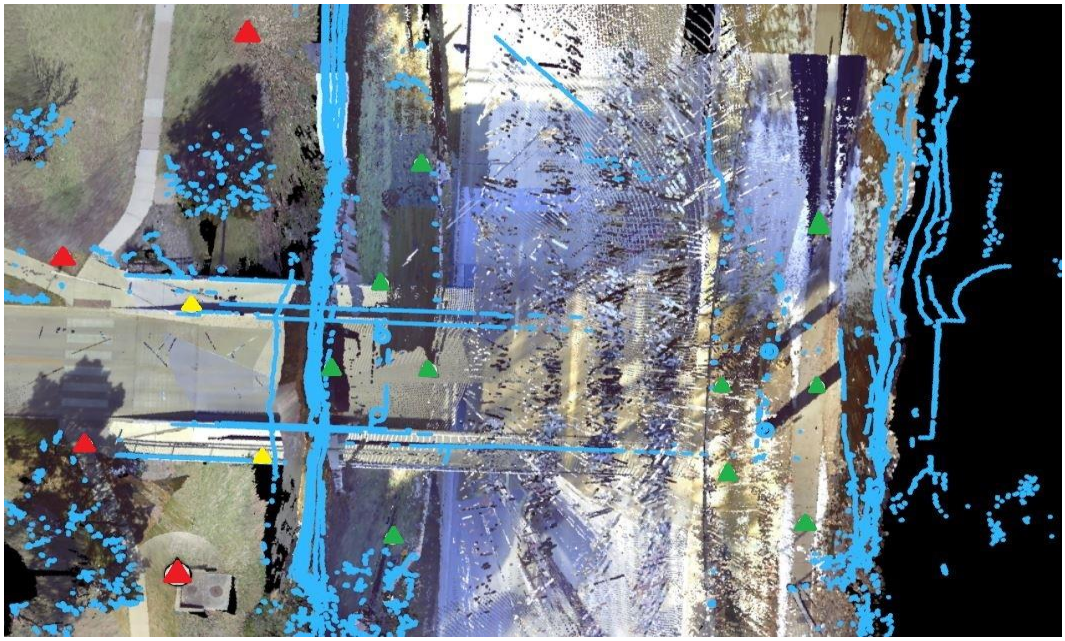

Figure 5.2: Scan locations

In the figure above, green triangles represent group 1, yellow triangles represent group 2 and red triangles represent group 3. Blue points show those points that are only visible in one scan file and have no overlap.

5.2.3 Office Work

5.2.3.1 Registration

Registration of the point clouds is the process of the combination of 3D data gained from scan worlds into one 3D system. The data collected from all scan locations was combined and registered into one common system. Through 3D registration, the 3D point cloud model was created of the bridge.

Scan registration was done using Autodesk Recap 360 and Trimble RealWorks. Both software support automatic registration. This feature uses geometric shapes and features that are common in different scans to automatically merge scans together. Integrity and quality of scan data depend greatly upon the accuracy of the registration process. Sans were taken so that each scan will have an ample area in common with next scan to accommodate the automatic registration process. Figure 5.3 shows the scan area overlap report generated at the end of the registration process. The report represented in Figure 5.3 only shows the scans included in scan group 1.

Figure 5.3: Scan overlap report

Another report generated by Trimble Realworks shows the coincident points (overlap area) of each scan separately with other scans. It also shows the confidence percentage, a measure of data integrity, for registration process and provides error range associated with scan registration. Figure 5.4 shows an example of such report generated for scan labeled as New_Project_Scan_10 in scan project with respect to other scans in group 1. The report shown in Figure 5.4 shows that for every scan the error in point cloud data is less than 2mm or 0.08 inches. Such precision makes laser scanner data very reliable for collecting bridge geometric data.

New_Project_Scan_010 - 9 Station(s) with Points in Common -

Object Name.	Cloud-to-cloud error.	Coincident Points (%).	Confidence (%)
New_Project_Scan_001	1.63 mm	47%	100%
New_Project_Scan_002	1.92 mm	61%	100%
New_Project_Scan_003	1.03 mm	57%	100%
New_Project_Scan_004	1.18 mm	73%	100%
New_Project_Scan_005	2.00 mm	36%	100%
New_Project_Scan_006	1.81 mm	37%	100%
New_Project_Scan_007	1.29 mm	47%	100%
New_Project_Scan_008	1.01 mm	40%	100%
New_Project_Scan_009	1.98 mm	59%	100%

Figure 5.4: Scan registration, accuracy report

5.2.3.2 Geometric Data Extraction and Validation

After the successful registration of scans into one coordinate system, the 3D point cloud model was created. Before the extraction of any geometric data, it is important to clean up the scans for any noise due to traffic and other interruptions. During scan process, scanner picks up points off of moving objects such as cars and pedestrians in some frames. However, due to 360-degree rotation of scanner at a slow speed, moving objects that are visible in each frame differ. Thus, these objects become noise to actual point cloud data. Autodesk Recap's noise removal tool "cleanup" was used to remove noise from project data. The cleanup tool automatically removes unwanted points such as accidental captures of moving vehicles and pedestrians from registered scans. Figure 5.5a and 5.5b shows 3D point cloud model of the bridge after noise removal.

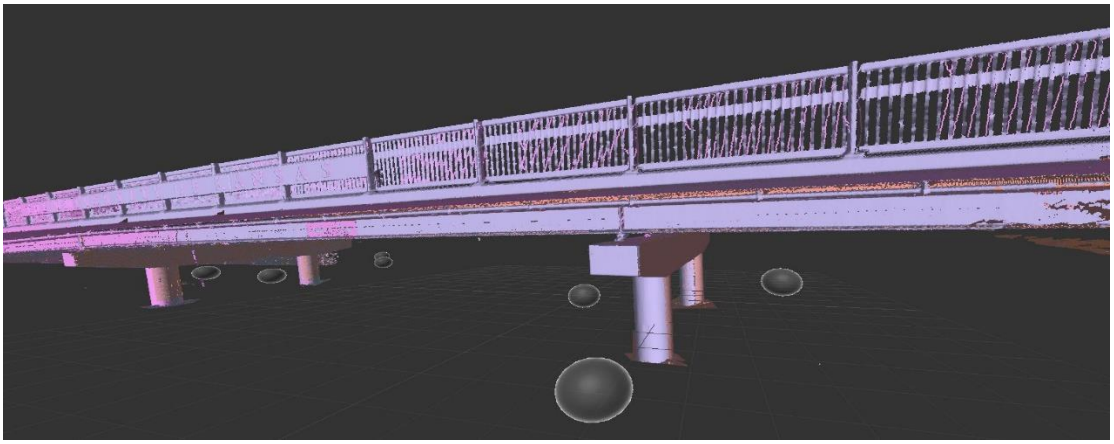

Figure 5.5a: Bridge model in scan colors

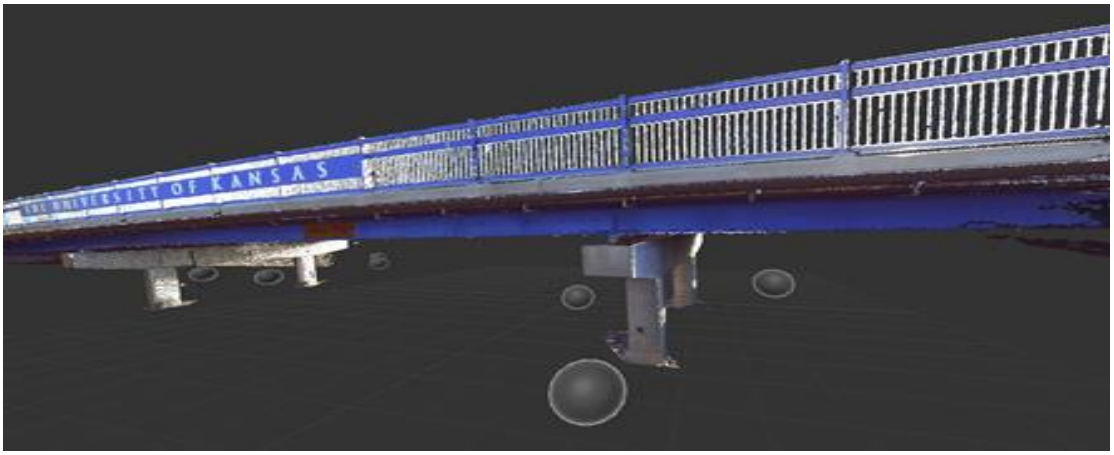

Figure 5.5b: Bridge model in true colors

The TX5 laser scanner has the capability to retain red-green-blue (RGB) values for each individual scan point so that the 3D point cloud model (Figure 5.5a) can be created in true colors. Another way to show scan points is to generate a model using intensity based color coding (Figure 5.5b). The intensity of a scan point is higher when the incidence angle is low. Also, the intensity will be high for points that are common in multiple scans.

After the completion of noise removal, geometric data was extracted from the point cloud model. NBI geometric data items (Table 3.1) were extracted from laser scan data as well as from actual construction drawings for the bridge. Comparison of these two set of values was used to validate the accuracy of scan data.

In order to extract data from point cloud model, ortho snap and surface snap features in ReCap 360 was used. Extreme care was observed to select the right point while taking measurements. Slightest error can result in the selection of a far-off point and mess up the measurement. In measurements with a high number of points clustered together, chance of snapping a point in a different layer is quite high. In such instance, RealWorks was used to cut a vertical plane through the model. This feature allowed to measure the scan points that lie on the cutting plane without interference from other scan points.

Table 3.1 demonstrate 16 NBI items that are associated with geometric measurements. Out of those items, skew was not taken into account as there was no evident data from construction drawings against which measurement error could be computed. Vertical clearance over bridge roadway was also not taken into account as there is no structure over the bridge.

Minimum vertical clearance was measured near north-eastern pier instead of center as the same measurement was given in drawings. Minimum inventory route vertical clearance was also measured at the same point. This point lies at the edge of the roadway on the west side of the bridge. This point represents the minimum vertical clearance for roadway and shoulders. Figure 5.6a shows the bridge plan and minimum clearance as shown in drawings and Figure 5.6b shows the same measurement from scan data. Minimum navigational vertical clearance was measured at the center of the underlying road (Figure 5.6c).

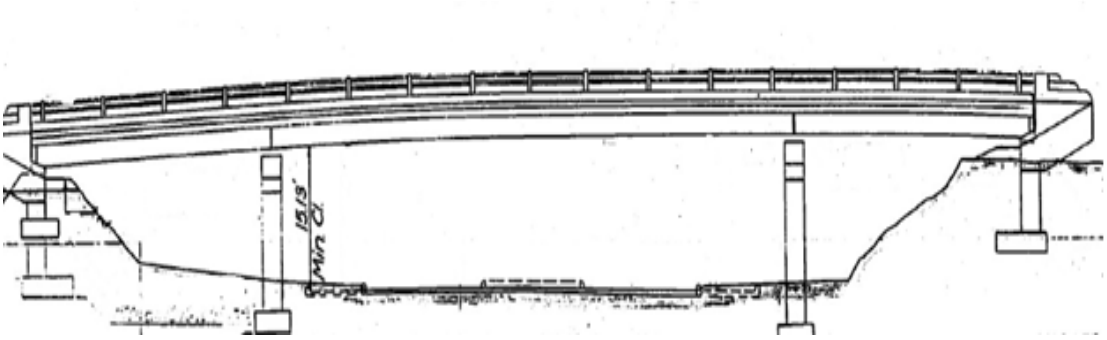

Figure 5.6a: Minimum vertical clearance as given in drawings

Figure 5.6b: Minimum vertical clearance from scan data

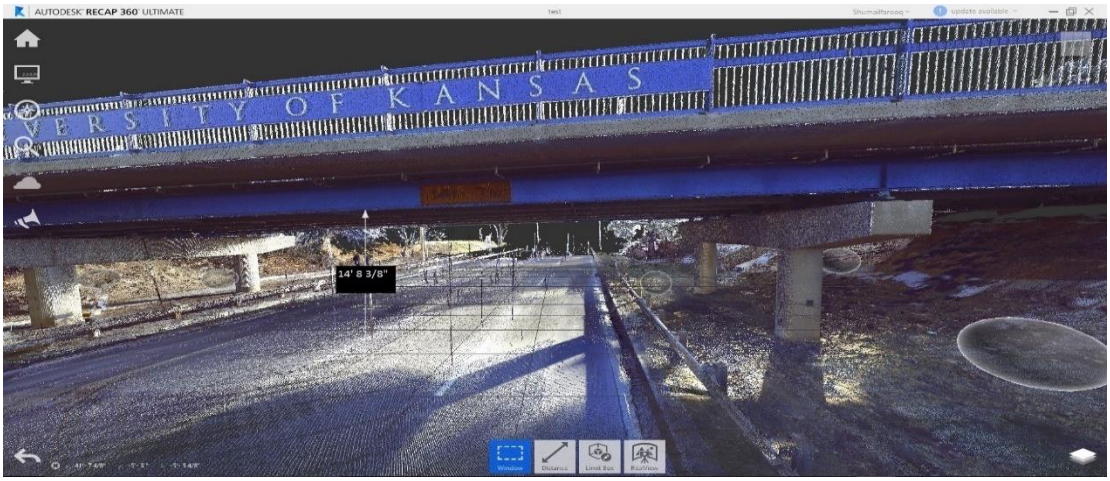

Figure 5.6c: Navigational vertical clearance

Minimum lateral clearance under the bridge was measured from the edge of curb to the first restrictive structure i.e. piers. Figure 5.7 shows the measurement obtained from scan data for minimum lateral under clearance.

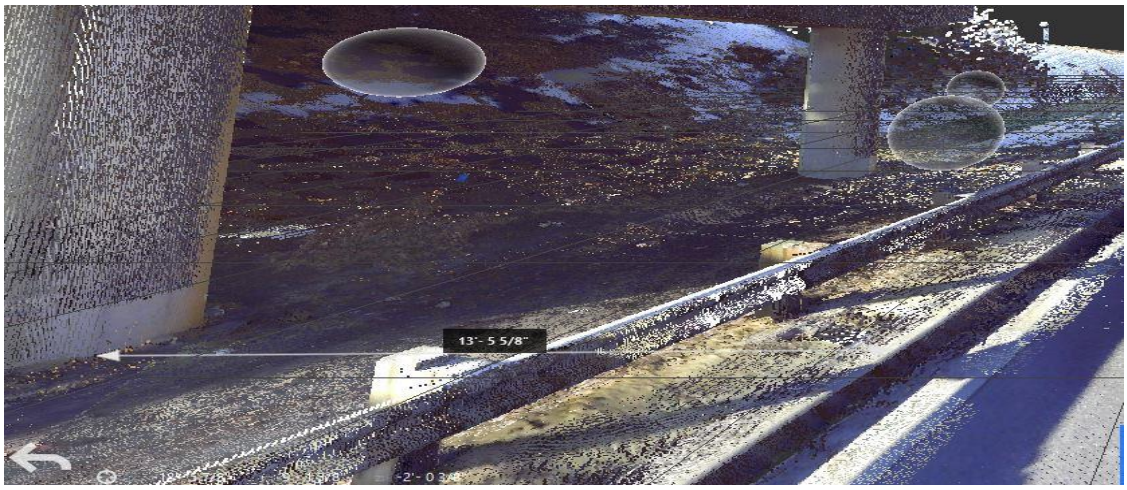

Figure 5.7: Minimum lateral under clearance on west side

Similarly, a measure was taken on the east side of the underlying road to demonstrate the minimum lateral under clearance on the east side. Figure 5.8 shows the measurement taken from scan data.

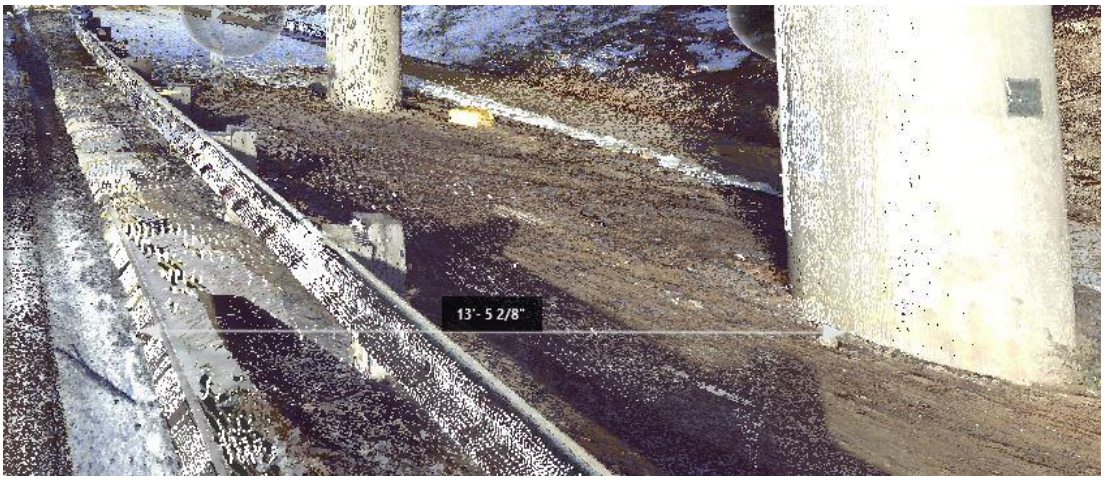

Figure 5.8: Minimum lateral under clearance on east side

Navigational horizontal clearance was measured from the centerline of the roadway to the edge of the piers. Figure 5.9 shows the demonstration of the results obtained from scan data.

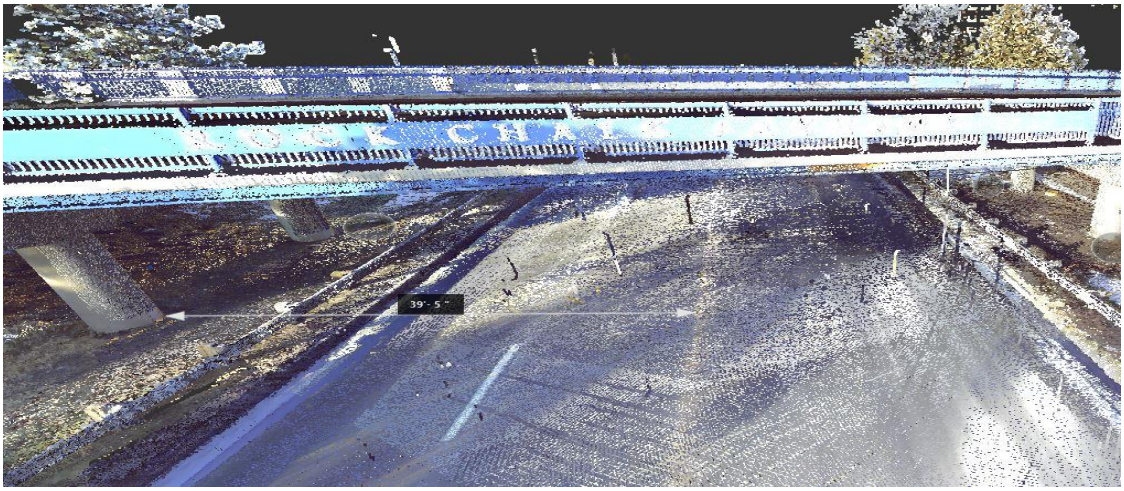

Figure 5.9: Navigational horizontal clearance

Inventory horizontal clearance was measured from curb to curb. Inventory horizontal clearance represents the width of underlying roadway including the shoulder. Figure 5.10 shows the measurement obtained from scan results.

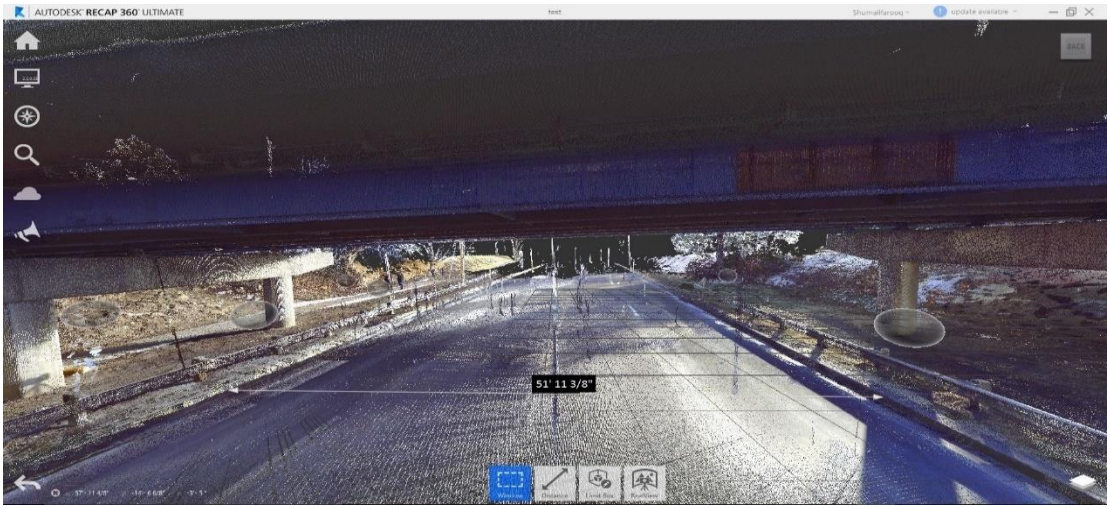

Figure 5.10: Inventory horizontal clearance

Figure 5.11 shows the horizontal clearance and lateral dimensions of underlying road and bridge structure as shown in original plan drawing.

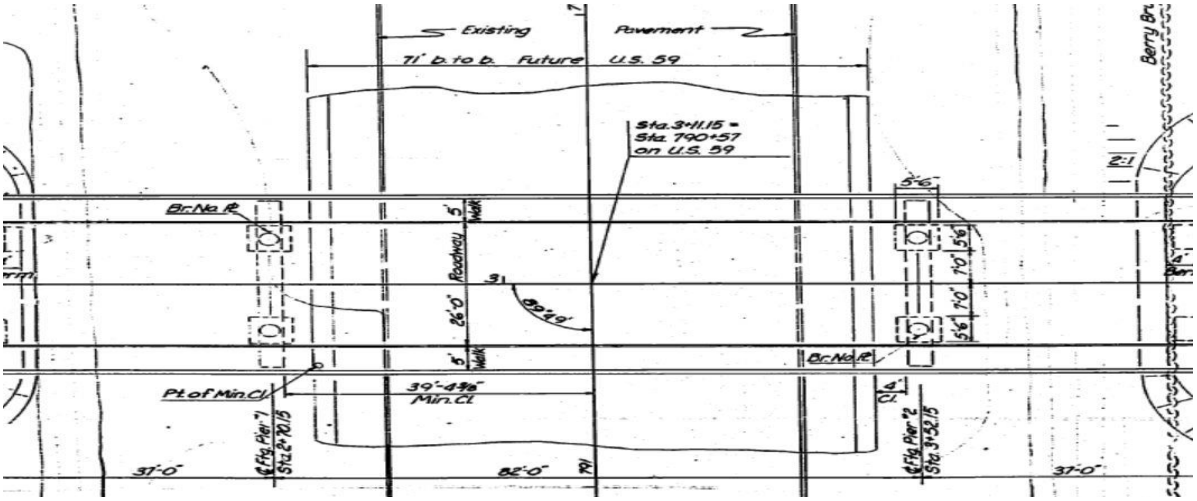

Figure 5.11: Horizontal clearance from construction drawings

Similar to above measurements, other items in Table 3.1 were measured using scan data and compared with values extracted from construction drawings.

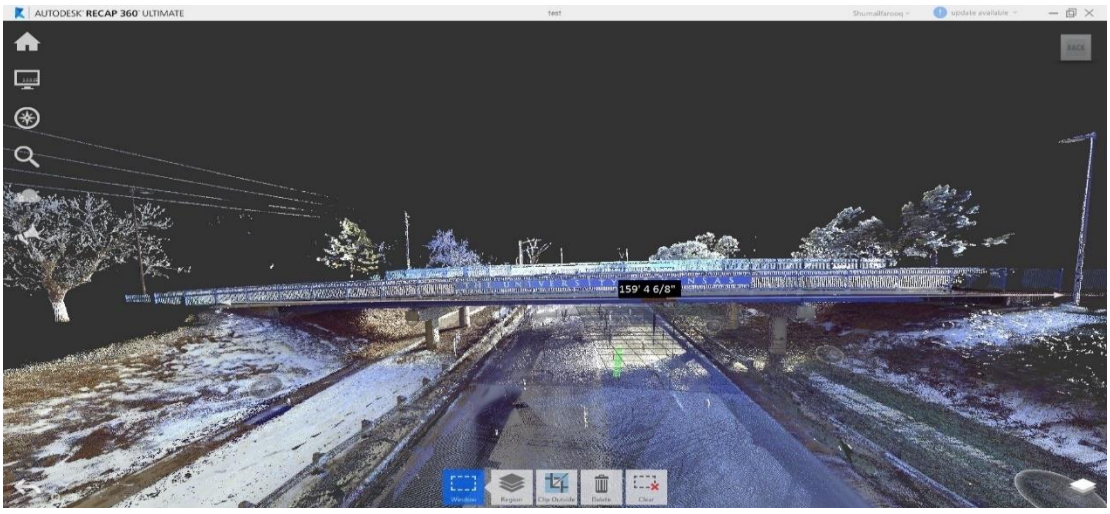

Figure 5.12a: Length of structure from scan data

End to end dimension of wearing surface from plan drawings is shown in Figure 5.12b.

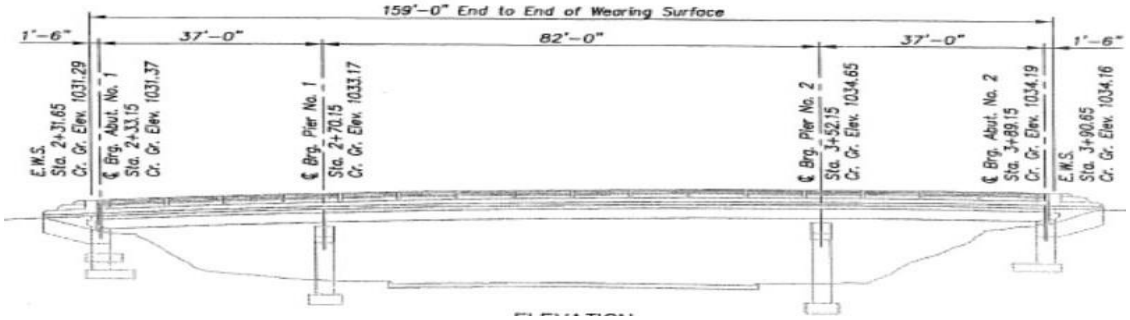

Figure 5.12b: Length of structure from drawings

The width of approaching road was measured for the Irving hill road approaching the bridge from the west side. East side road was close to the intersection and thus its width was not considered. Figure 5.13 shows the measurement obtained from scan data.

Figure 5.13: Width of approaching road

Next item on the list was the width of bridge roadway. Measuring the roadway width was tricky in true colors as the shadow of sidewalk medians hindered in capturing the desired points. The measurement was taken along an expansion joint to assist in capturing the desired points. Figure 5.14a shows the measurement.

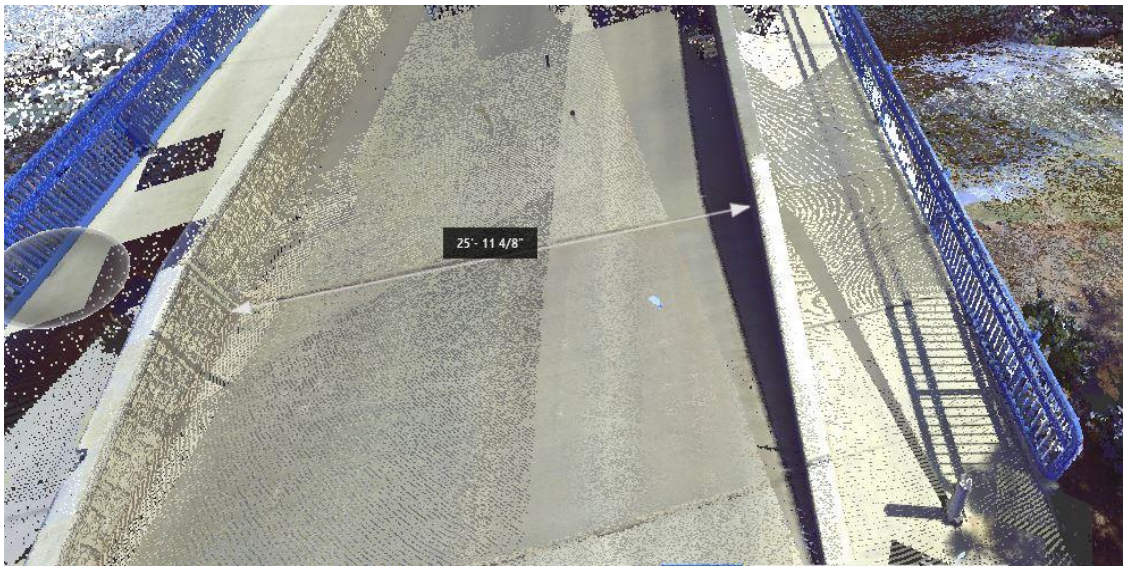

Figure 5.14a: Bridge roadway width from scan data

Figure 5.14b shows the width of bridge roadway from plan drawings.

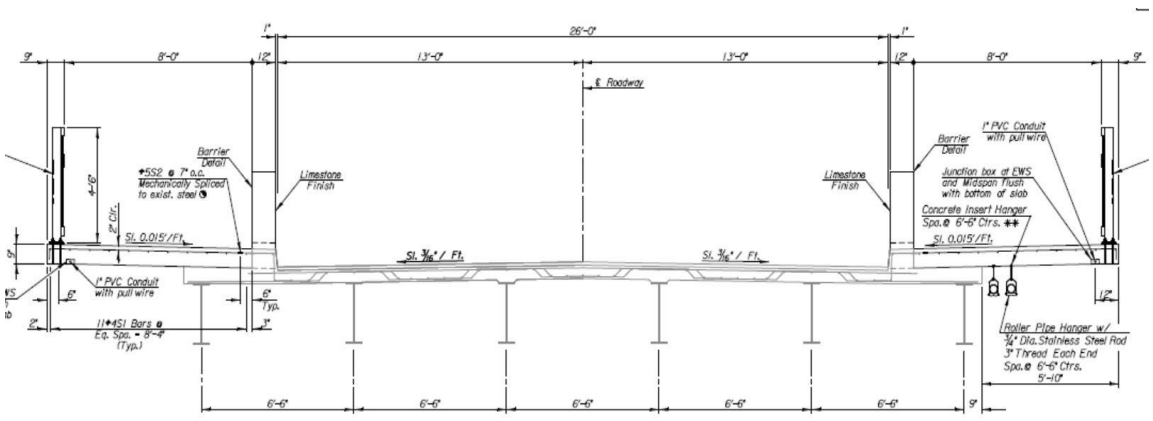

Figure 5.14b: Bridge roadway width from drawings

Figure 5.15 shows the measurement for the length of the maximum span as obtained from scan data. The length was measured using the center of the pier as a reference. The measurement from plan drawings is evident in Figure 5.12b.

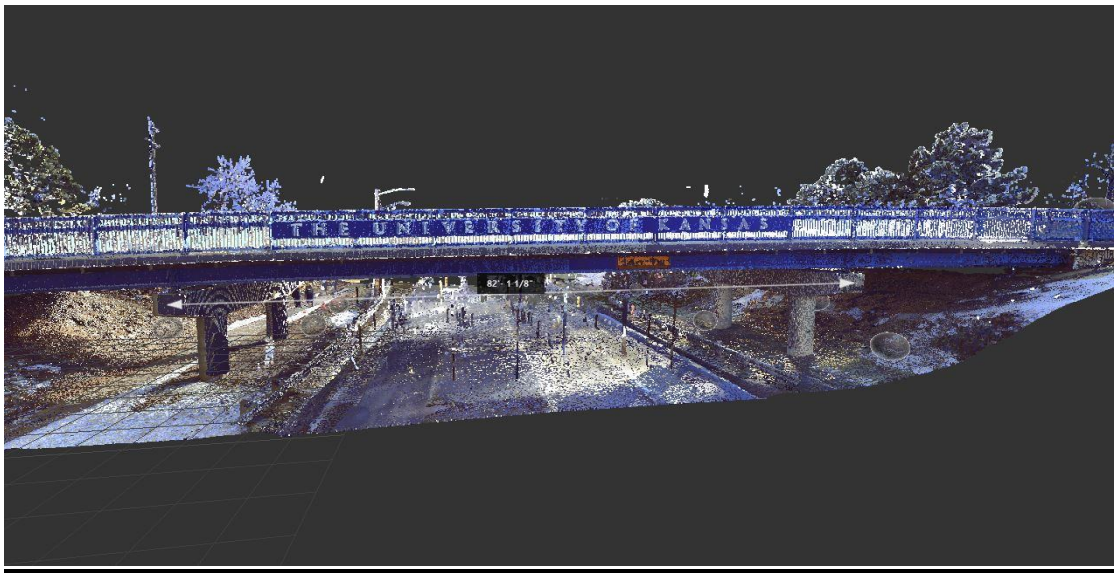

Figure 5.15: Maximum span length

There are three set of drawings for this bridge. Originally, the bridge was constructed in 1965 and rehabilitated in 2005. In 2015, an improvement was conducted to increase the width of the bridge deck. After improvements, the bridge deck width was increased from 39 feet to 45.5 feet. Sidewalks on both sides of the bridge were widened from 5 feet in the original plan to 8 feet (Figure 5.14b). Figure 5.15 shows the measurement from scans for deck width.

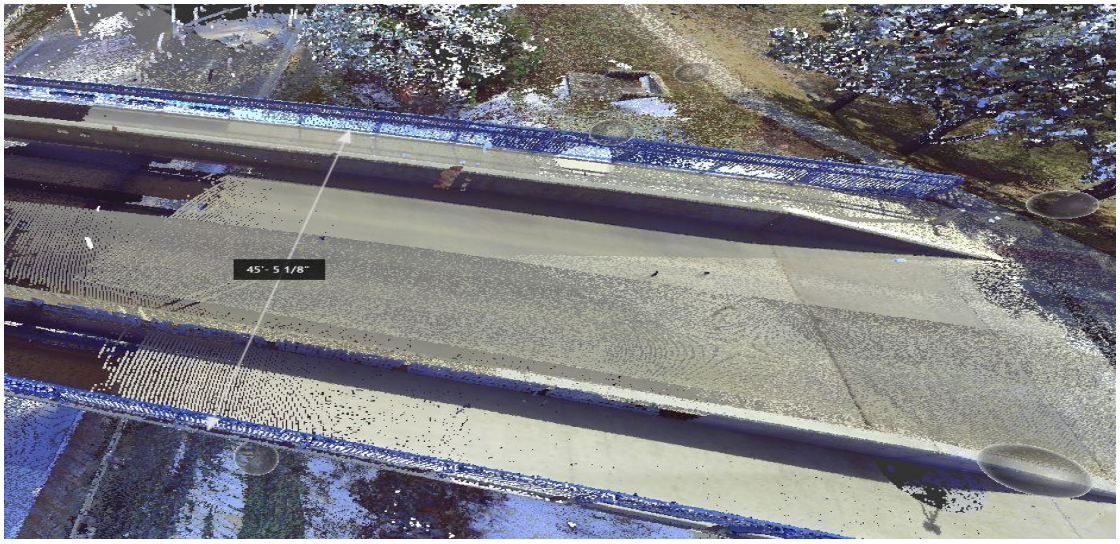

Figure 5.16: Deck width, out-to-out

Figure 5.17 shows the width of the sidewalk as measured on the north side of bridge roadway.

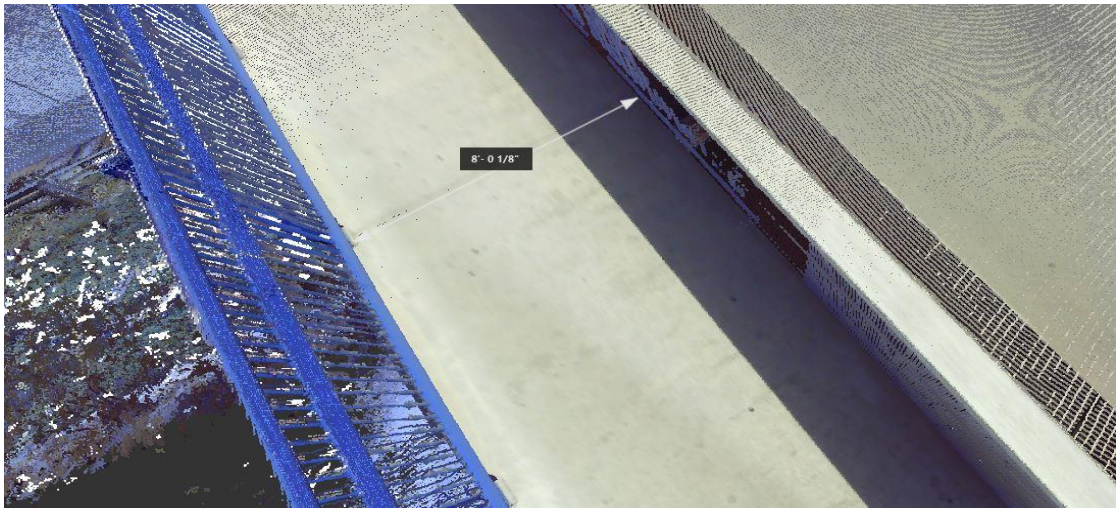

Figure 5.17: Width of sidewalk from scan data

After the extraction of all the data from scans and construction drawings, a comparison was made to determine the error in each measurement. Computed error was compared with allowable error range provided by NBI (Table 3.1). Results are shown in Table 5.1.

Table 5.1: Results of Data Validation

Item Name	NBI Precision Requirement (Feet)	Measurement from as-built Drawings (Feet)	Measurement from Scan Data (Feet)	Difference (Feet)
Structure Length	0.3275	159.00	159.15	+0.15
Maximum Span Length	0.3275	82.00	82.09	+0.09
Side Walk Width	0.3275	8.00	8.01	+0.01
Deck With, Out to Out	0.3275	45.5	45.512	+0.012
Minimum Lateral Under Clearance (West)	0.3275	13.50	13.47	-0.03
Minimum Lateral Under Clearance (East)	0.3275	13.50	13.43	-0.07
Inventory Horizontal Clearance	0.3275	52.00	51.94	-0.06
Minimum Vertical Under Clearance	0.0327	15.13	15.11	-0.02
Navigational Vertical Clearance	0.3275	14.58	14.69	+0.11
Navigational Horizontal Clearance	0.3275	39.36	39.42	+0.06
Width of Bridge Roadway	0.3275	26.00	26.95	-0.05
Width of Approaching Roadway	0.3275	27.00	26.89	-0.11

Error in each measurement was less than the NBI specified limit. All 15 items met the required accuracy. Although, structure length and maximum span length showed much bigger deviations

than other items. This deviation is a result of “noise” in scan data due to moving cars on the road underneath the bridge.

5.3 Crack Detection and Crack Width Computation Using Two-Dimensional Photographs

The final part of this research is a proposed crack detection and crack width computation process using photographs. This method uses photographs taken by a high-resolution camera and implements MATLAB codes to detect cracks. Data collection for this part was done simultaneously with the scanning process. Components of the bridge structure that showed fatigue were photographed closely. Care was observed while taking photographs to keep the camera perpendicular to the center of the area being photographed. This particular detail is important to the accuracy of crack width computation. This methodology is a modified version of crack detection algorithm for pavement cracks discussed by Gopalakrishnan et al. 2016.

The Irving Hill bridge was used as a test subject for this part of research as well. The bridge has been remodeled and repaired in recent past, most of the cracks on structure surface are sealed off. By careful observation, two blocks (southwest pier and bottom of the deck) of the bridge structure were selected for analysis. Each of these blocks contains sealed or open crack(s). The results of crack width analysis will be unable to provide any verdict on bridge health for this particular case as most of the cracks have been sealed and the bridge has been repaired recently. Yet this data is considered adequate to provide proof-of-concept for proposed methodology.

The objective of this proof-of-concept research project was to develop an image-based crack-detection approach for the reliable detection and of cracks from acquired 2D images. The developed approach takes advantage of the spatial distribution of crack pixels and works on each pavement image block of 100 by 100 pixels. After completing the crack-detection process, the width of each crack segment is computed to determine severity.

5.3.1 Shape-Based Crack Detection Approach

This research proposes a shape-based crack detection approach, taking advantage of the spatial distribution of crack pixels. This approach works on each image block of size 100 by 100 pixels and consists of two stages:

1. Image filtering
2. Crack extraction

5.3.1.1 Image Filtering

Considering the fact that crack pixels have relatively lower intensity values compared to non-crack pixels in the image, it is necessary to first design a filter to remove non-crack pixels for each raw image, $RawImage^{(i)}$. The filter is defined as follows

$$ProcessedImage^{\{(i)\}(x)} = \{1, \text{ if } RawImage^{(i)(x)} < p * n^{(i)}. \quad \text{else, } 0\} \qquad (1)$$

where $RawImage^{(i)(x)}$ and $ProcessedImage^{(i)(x)}$ represent the image intensity at position x in input photograph, $RawImage^{(i)}$, and output, $ProcessedImage^{(i)}$, respectively; $^{(i)}$ is the mean intensity value of input block $RawBlock^{(i)}$; and parameter ‘p’ depends on the histogram analysis of raw image.

Once the filter is applied it will distinguish the crack pixels and non-crack pixels in processed photograph. To demonstrate the defined filter, an example is presented below. Image used in below example shows underneath of bridge deck. A sealed crack was spotted underneath deck which was photographed for test purpose.

Figure 5.18 shows the true image as taken using a high-resolution camera. The size of the image was reduced to 100x100 pixels for simplification. Large images can make computation difficult and increase the error probability due to lighting conditions. The image was resized using MATLAB command **imresize(I, [100 100]),** where I represent said image.

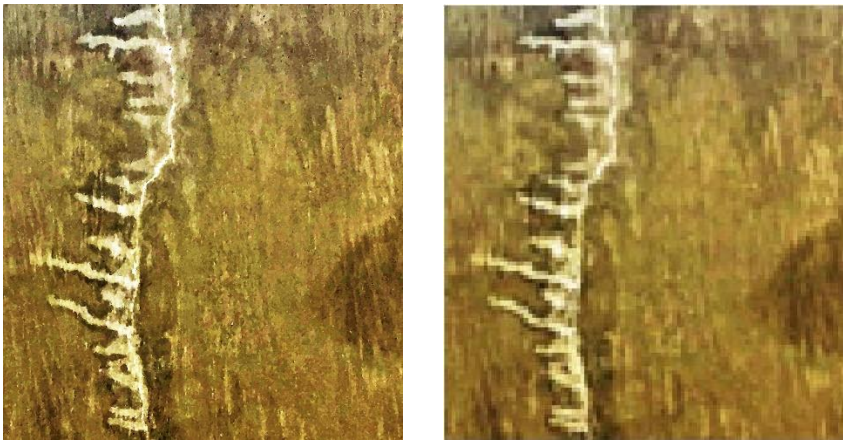

Figure 5.18: Raw image(left) vs resized image(right)

Before the filter can be applied it is important to perform a histogram analysis to determine the value of parameter ‘p’. This parameter will act as an intensity threshold to remove non-crack pixels when applying the filter defined in equation 1. The histogram provides a graph representing intensity value for all pixels in a given image. By closely observing histogram, we can determine at which value the no-crack pixels and crack pixels can be separated from each other. In order to create a histogram, the image is needed to be in grayscale format instead of red

green blue(RGB) format. MATLAB command **rgb2gray()** is used to convert the image in Figure 5.18(right) into a grayscale image. Figure 5.19 shows the resulting image.

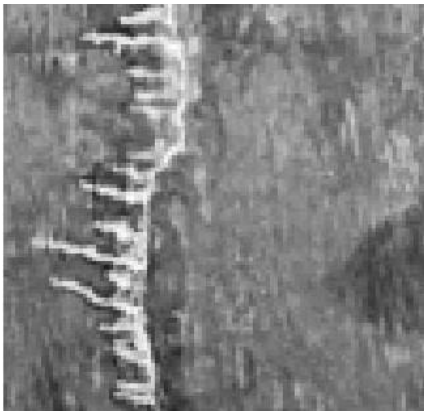

Figure 5.19: Grayscale image

Once the image is converted to the grayscale format, the histogram for the image is created (Figure 5.20). MATLAB command **imhist(gray)** was used to create the histogram, where gray represents an image in grayscale. Figure 5.20 represents the histogram for the test image.

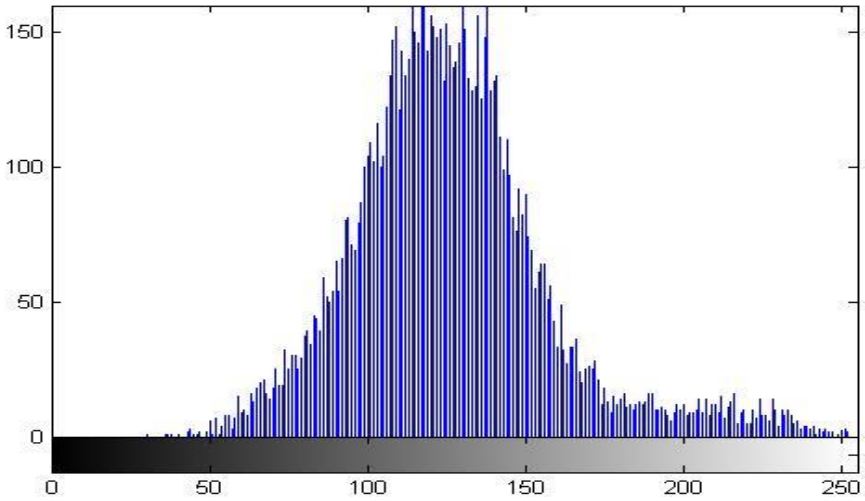

Figure 5.20: Histogram

the x-axis of this graph represents intensity values also know as ‘bins’ in MATLAB coding language. MATLAB automatically plots a histogram for grayscale images using 256 bins. Color bar at the bottom of the graph represents the bin value in correlation with gray-scale with black having a value of 0 and white having a value of 256. To simplify the histogram, a manual value can be provided to color bar associated with a histogram which will pair the pixels that correlate to same value range on specified color bar. A scale of 10 was provided using command **imhist(gray,10)** in MATLAB, resulting histogram is shown in Figure 5.21.

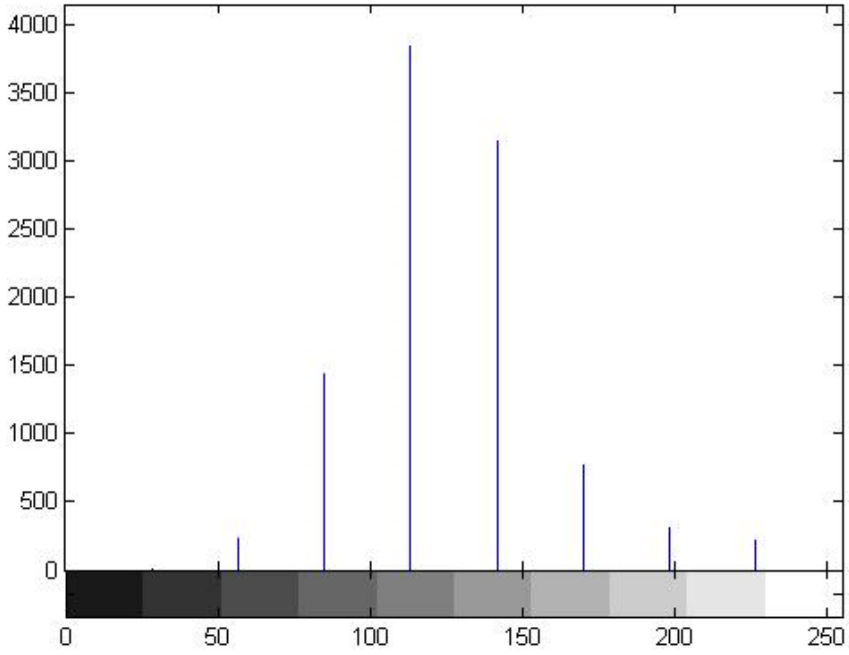

Figure 5.21: Refined histogram

By analyzing histograms in Figure 5.20 and 5.21, a range of 0.65 to 0.88 was determined for parameter ‘p’. An appropriate empirical value for ‘p’ was determined to be 0.7 by hit and trial method.

Using the value determined by histogram analysis, filter defined in equation 1 can be implied on test image as follow

ProcessedImage = im2bw(GrayscaleImage, 0.7)

Where processed image is the output of image filter, **im2bw()** is MATLAB command used, Grayscale Image is image shown in Figure 5.19 and 0.7 is the value of parameter 'p'.

Output *ProcessedImage* is a binary image, where white and black pixels correspond to possible crack pixels and non-crack pixels, respectively. Results of the performance of filtering are shown Figure 5.22. An observation can be made from Figure 5.22 that the local filter has the capability to extract crack pixels, although it introduces some noise from structure textures.

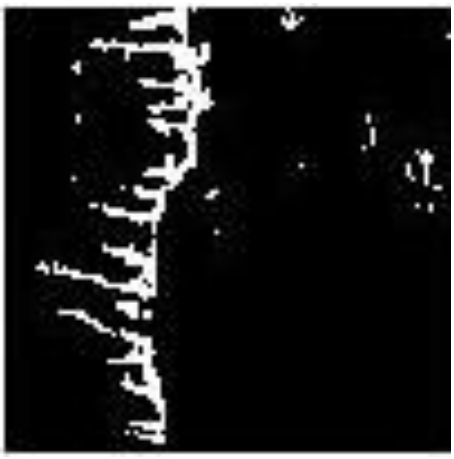

Figure 5.22: Filtered image

5.3.1.2 Crack Extraction

Because the local filter introduces some noise from structure texture when extracting crack pixels, we need to develop a major component extraction approach to refine crack pixels from all possible crack pixels.

For removal of minor components, MATLAB function **bwareaopen()** was used. The details are given as follows:

RefinedImage = bwareaopen(ProcessedImage; 15)

This MATLAB command aims to remove minor connected components whose sizes are smaller than 15 pixels. MATLAB command is applied for the minor component removal approach on the filtered binary Image as shown in Figure 5.23 (left) and display the output image in Figure 5.23 (right).

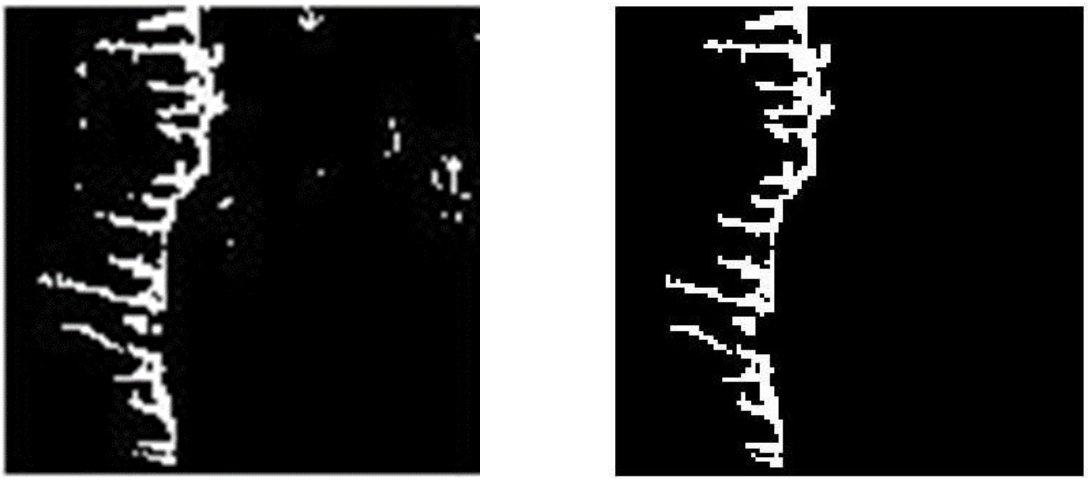

Figure 5.23: Minor component removal; input image (left) and output image (right)

5.3.2 Crack Width Computation

After detection of the crack segment, average crack width was computed to determine the severity of crack. For this purpose, a different image is used. Test image used during crack detection process shows a sealed crack. Due to the applied repairs, it is not possible to determine the actual width of crack. For this reason, a different image showing an open crack was used to demonstrate crack width computation. Image used shows a crack on the southwest pier of the bridge. Before photographing the crack, a rectangle of known parameters was created around the crack using tape. This was done to determine the width of the area visible in the photograph. The width of the image is 12”. Test image for crack width computation is shown in Figure 5.24.

Figure 5.24: Test image for crack width computation

In order to compute crack width, it is necessary to detect and extract the crack component using methodology discussed in the previous section. Figure 5.25 shows the histograms for the image shown in Figure 5.24.

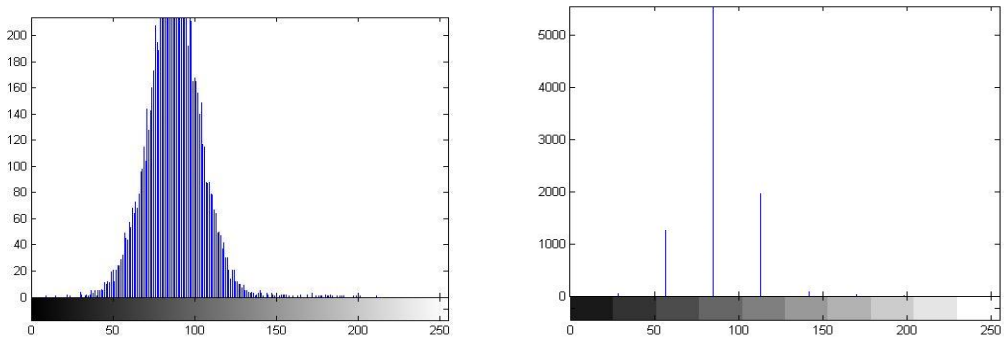

Figure 5.25: Histogram; Unrefined(left), Refined(Right)

From histogram analysis, the value of 'p' is determined to be somewhere between 0.4 to 0.8. The reason for selecting a larger range is to include crack pixels that might have less intensity due to lighting behavior. This will prevent any discontinuity in detected crack. After testing different values, 0.51 was considered to be most suitable. Figure 5.26 (left) shows the image after applying the image filter defined in equation 1. Figure 5.26 (Right) shows the image after removal of smaller components. As the size of crack is really small and texture noise is considerably large, a factor of 30 was used to extract crack component. Components with an area of fewer than 30 pixels were removed.

Figure 5.26: ProcessedImage with texture noise(left) and ProcessedImage after noise removal(right)

Average crack width can be defined as follows

$$AveCrackWidth = \frac{\sum (ymax - ymin)}{n} \quad (2)$$

where y_{max} represents max crack width for given crack component and y_{min} represents minimum crack width for given crack, n represents number of crack components (applicable in the case of non-continuous cracks).

MATLAB does not have any function/command to compute the average width of image component in pixels. In order to compute the width of crack, the author wrote a MATLAB code which returns maximum and minimum widths of the crack component shown in the image above. Code script is given below.

```
I = imread(ProcessedImage); %Reads the image
image(I);
CrakWidth = edge(I); %detects edges in the grayscale image or binary image
[r1,c1] = find(CrackWidth);
spy(CrackWidth);
x2 = max(r1);
x1 = min(r1);
X = x2 - x1
y2 = max(c1);
y1 = min(c1);
Y = y2 - y1
imshow(Crack Width);
```

where x1 represents minimum height value in pixels, x2 represents maximum height in pixels, y1 represents minimum width in pixels and y2 represents the maximum width in pixel. r and c represents rows and columns, respectively. Y represents width of crack and X represents height of crack.

The code starts by reading the ProcessedImage as shown in Figure 5.26 (left) and defines it as image I. In the next step, **edge()** command is used which detects the edges of crack components as shown in Figure 5.27. After that, a graph is plotted for edge points of the crack component using matrix [r1, c1]. After that **spy()** command is used to determine sparsity pattern of defined matrix [r1, c1].

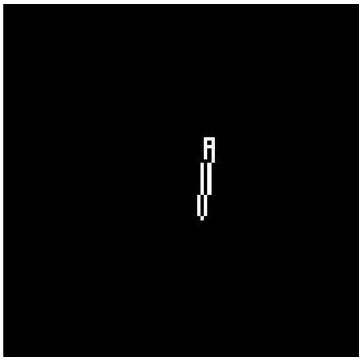

Figure 5.27: Edge detection for crack component

Once sparsity pattern is determined for the crack component, **min()** and **max()** commands are used to compute values of x2, x1, y2, y1 which represents maximum height pixel value, minimum height pixel value, maximum width pixel value and minimum width pixel value, respectively. Next, we use equation 2 to compute average crack width for the crack component.

The code returns a value of 22 pixels for the height of crack and 4 pixels for the width of crack. Since the crack is not oriented vertically the value of crack width computed is not accurate. In order to correct this error, MATLAB command **regionprops()** was used to determine the orientation of crack which returned a value of 83.66 degrees. Next **imrotate()** was used to rotate the image to fit vertical orientation. Figure 5.28 shows test image after rotation.

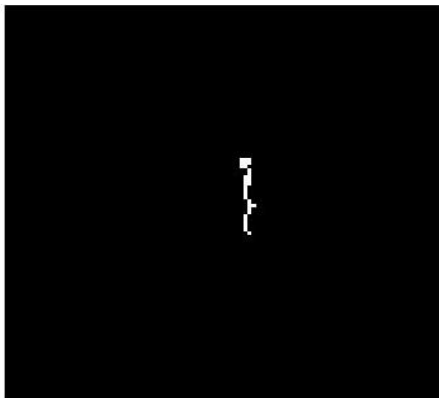

Figure 5.28: Image after rotation

After running the width detection code on rotated image, the width of the crack component is calculated to be 3 pixels. From data collection, it is known that width of the image block is 12” and test image width is divided into 100 pixels. This means that each pixel is 0.12” wide and width of crack is 0.12 x 3 = 0.36” or 0.9 cm.

5.4 Summary

Chapter 5 discusses the proposed methodology in detail. This chapter discusses the methods implemented to collect and analyze data in order to demonstrate the research framework. The chapter is divided into two major sections, section 5.2, and section 5.4. First section 5.2 describes complete data collection using a TX5 laser scanner. Section 5.2 also describes the analysis techniques implemented on laser scanner data to create point cloud model of the bridge and extract geometrical data. Section 5.3 is focused on image-based crack detection and crack width computation. For crack detection, data was collected using the high-resolution camera and MATLAB functions were used to extract crack blocks from photographs. After that, a MATLAB code was developed to compute the widths of detected cracks.

Chapter 6: Key Findings and Summary

6.1 Introduction

This chapter presents the key findings of the research project. Results for data validation and accuracy are discussed for the 3D point cloud model. Also, the results obtained from crack detection and crack width computation are discussed. This project also contains a section describing the lessons learned from data analysis and results.

6.3 Key Findings

This section discusses the results obtained as a result of data analysis put forth in research framework explained in Chapter 4 and Chapter 5 of this thesis. Data analysis was conducted in two parts, laser scan analysis and crack analysis. The objective of laser scanner analysis was to validate the accuracy of geometric data extracted from point cloud model against the requirements provided by the NBI. On the other hand, crack analysis was a proof of concept research project. No data was available to validate the results obtained from data analysis. The objective of the crack analysis was to demonstrate the workings of the proposed image-based crack detection technique.

Table 6.1: Error Percentage in Laser Scanner Data

Item Name	Measurement from as-built Drawings (Feet)	Measurement from Scan Data (Feet)	Difference (Feet)	Error %
Structure Length	159.00	159.15	+0.15	+0.09
Maximum Span Length	82.00	82.09	+0.09	+0.10
Side Walk Width	8.00	8.01	+0.01	+0.10
Deck With, Out to Out	45.5	45.51	+0.012	+0.02
Minimum Lateral Under Clearance (West)	13.50	13.47	-0.03	+0.22
Minimum Lateral Under Clearance (East)	13.50	13.43	-0.07	-0.50
Inventory Horizontal Clearance	52.00	51.94	-0.06	-0.11
Minimum Vertical Under Clearance	15.13	15.11	-0.02	-0.13
Navigational Vertical Clearance	14.58	14.69	+0.11	+0.75
Navigational Horizontal Clearance	39.36	39.42	+0.06	+0.15
Width of Bridge Roadway	26.00	26.95	-0.05	-0.19
Width of Approaching Roadway	27.00	26.89	-0.11	-0.40

1. Data collected using laser scanner showed high accuracy. Results obtained from scan analysis showed an error in measurement in the range of +/- 0.15 feet with 8 out of 15 measurements showing an error of less than or equal to +/- 0.07 feet. Table 6.1 summarizes the data analysis results and error % of the data collected using a laser scanner. The error % of each measurement is less than 1%.

2. 3D laser scanner data meets the accuracy specified by NBI. NBI accuracy requirement for most of the geometric data is +/- 0.3275 feet. Table 6.1 shows the results for each NBI item that is related to geometric data for bridge inspection. Error computation for all items is in accordance with the requirements put forth by NBI. The obtained results provide a conclusive proof that laser scanner data is reliable for bridge inspection process. In addition to high accuracy, laser scanner provides time efficiency over traditional surveying techniques with less manpower and no interruptions to traffic flow.

3. Workable crack analysis process using digital photographs. Section 5.2 of this thesis shows a successful example of crack detection in bridge structure using 2D photographs and MATLAB codes. Also, section 5.2 gives an example of crack width computation with ambient accuracy to determine the severity of crack damage in the bridge structure.

6.4 Lessons Learned

1. Low incidence angle is desirable. After the comparison of data by the laser scanner with design drawing data, we can say that terrestrial laser scanners are meeting the general engineering requirements. The accuracy of the measurements is dependent on the incidence

angle between the laser beam and the object's normal. Low incidence angle is preferable to gather more accurate data. The distance of the object from laser scanner position can also be a source of error. Environmental conditions and moving objects can cause more data noise in final point cloud data.

2. The speed and accuracy of a laser scanner is an advantage over conventional tools. The main objective of using laser scanner as a principal surveying tool is to pace up the surveying process. Ability to gather millions of data points per second with an accuracy of $1/100^{th}$ of a foot gives a vast advantage on mega projects. This results in an improved productivity level for surveying tasks. Similarly, in bridge inspection process, use of laser scanners provide a rapid data collection process with minimum manpower and improved accuracy. The accuracy of scan data can also be improved further by setting the scanner at the smallest possible resolution. This will shorten the spot size of the laser scanner or in other words shorten the width of the laser beam, thus improving the accuracy at a point-to-point level.

3. Uninterrupted traffic flow. Laser scanner also provides an added advantage of uninterrupted traffic and pedestrian flow during data collection process. This is a clear advantage over traditional equipment in the ground profile mapping of bridge or roadway project. Also, laser scanners reduce the direct labor cost and increase the safety of collection efforts.

4. There is room for improvement in crack analysis techniques. Health assessment of bridges is crucial in determining the capability of the bridge to perform at the desired level. Detecting the cracks in bridge structure and analyzing the severity of crack damage is an integral part of bridge health assessment. Advancements are still being made in the development of accurate and reliable image-based crack detection and classification algorithms. There is a need for the

development of automated, low-cost crack detection algorithms that could be implemented for cost-effective and continuous health monitoring and management of bridge structures. The proposed algorithm represents an effective way of detecting cracks and computing crack width, but there is room for improvement.

6.4 Summary

Chapter 6 discuss the key findings of this research project. The results obtained from analysis discussed in Chapter 5 are discussed in detail in this chapter. This chapter also provides the key findings and lessons learned from the research conducted during this thesis.

Chapter 7: Conclusion and Future Studies

7.1 Introduction

This chapter concludes this thesis by providing an overview of performed tasks and discussing the essence of research conducted over the course of project life cycle. This chapter will conclude the findings of the accuracy of laser scanner implications for bridge inspection and assessment and the image based crack detection and width computation method. This chapter will also discuss the limitations of research methodology and challenges faced during the course of the research project. Chapter 7 will conclude by discussing the future work to further extend and improve the research discussed throughout the thesis.

7.2 Conclusion and Contributions

Research presented in this thesis comprises of a two-phase project to demonstrate an advanced mean of bridge inspection and assessment. The research was initiated with a clear goal of assessing the implementations of the laser scanner and 2D photographs in the process of bridge inspection and assessment. By virtue of extensive literature review on current bridge inspection process, a framework was created to validate the use of laser scanner technology for gathering bridge inspection data show the accuracy of gathered data by comparison with actual construction drawings of the bridge.

After analyzing the data gathered by the laser scanner and comparing the results, the author concludes that the accuracy of point cloud data is in accordance with NBI requirement for

specific geometric data items as listed in NBI bridge inspection checklist. Laser scanner also provides an added advantage of time efficient surveying process than traditional equipment with less manpower used and no interruptions to traffic flow.

The results described in Chapter 5 shows that the error ratio in geometric data extracted from point cloud data gathered by laser scanner is in the range of 1% to 2%. The scans taken for this study were of a moderate resolution. If need be, the accuracy of laser scanner data can be further enhanced by increasing the resolution of the laser scanner.

The content in this thesis also presents a framework for an image-based crack detection and crack width computation algorithm. The author was able to successfully detect the cracks from photographs of the bridge structure and compute the width of cracks. Cracks width is an important parameter for determining the severity of damage due to fatigue in concrete bridges and assessing the health of bridge structure.

The study concludes that the data collected by laser scanner has an accuracy which meets the required accuracy listed by NBI for bridge geometric data. Also, the proposed image-based crack analysis technique has the capability of providing satisfactory results for assessing the health of bridge structure.

This research will contribute to the ongoing transition of bridge inspection process from conventional methods to more automated and efficient techniques. There is a critical need to update the current bridge inspection process from a paper-based format to a digital format.

7.3 Limitations

Even though the research discussed in this thesis has yielded positive results, it has a few limitations in its implication. 3D laser scanners provide an advantage in speed and accuracy but there are still some limitations to its use. The laser scanner cannot work properly in adverse conditions i.e. rain, fog, mist or adverse wind. Moisture in the air can temper with the laser beam and introduce 'false' points in the scan. High incidence angle can also hinder the accurate data collection process. In addition, a surface with a shallow layer of water, due to its high reflectivity, may cause noisy point cloud data. In the case of excessive scan noise, more time is required to filter the noisy points.

Another limitation to laser scanners is the surrounding environment, the scanner can only capture objects that are in clear line of sight of its laser beam. Excessive vegetation around the base of a bridge pier can make it impossible to properly capture such features. The bridge studied for this research had vegetation in close proximity to the structures which made it difficult find ample common area between the scans taken from underneath the bridge and those taken from above the bridge. A set of extra scans had to be taken in order to get better registration results.

The image-based algorithm described in this research is limited in distinguishing between cracks and texture irregularities. Irregularities in the concrete surface such as uneven texture can appear as indistinguishable from crack pixels making it a semi-manual process. Also, the accuracy of the width computation has an error of +/- 1-pixel width.

Bridge inspection techniques presented in this research are limited to assessing the health of structure on the surface level. Any damage or deficiencies on the sub-surface level cannot be assessed using the proposed framework.

7.4 Future Studies

3D laser scanners will be used more widely for the highway/bridge engineering survey applications in structural projects. Some scanning processes are combined and used with conventional survey methods for measurements, target acquisition or elevation differences. Also, laser scanners can detect the trend of movement or settlement of the whole structure by comparing the scanned 3D models captured at different times.

1. Development of Common Data Format. There is a need to conduct more studies to find a way to incorporate automated techniques in bridge inspection process. One way is to bridge the gap between bridge information modeling (BrIM) and 3D laser scanner by creating a common format for better exchange of data.

2. Use of Ground Penetrating Radar (GPR). Another study can be conducted to integrated terrestrial laser scanners with GPR. GPR systems are used to investigate the sub-surface properties of a structure. Integration of GPR in bridge inspection can help assess the inner damages to a structure and analyze the conditions of foundations and sub-surface parts of piers.

3. Upgrade of Crack Analysis Techniques. The image-based crack detection process is very fundamental at this stage, although many studies have come forth in recent years refining the process of crack detection and width computation, there is still room for major improvements. A

study can be conducted to develop a software to perform image-based crack detection and width computations on site. This will help to speed up the bridge inspection process and eliminate the need for assessing individual photos in the laboratory.

References

New York State Department of Transportation (2008). "Fundamentals of bridge maintenance and inspection", New York.

Cihan M. (2011). "Evaluation of laser scanning technology for bridge inspection", thesis, presented to Drexel University in partial fulfillment of the requirements for the degree of Master of Science in Civil Engineering.

American Society of Civil Engineers (2017). "Infrastructure report card." MUD history, < www.infrastructurereportcard.org> (April 20, 2017).

National Bridge Inspection Standards 23 C.F.R. §650.303- §650.313 (2004).

American Association of State Highway and Transportation Officials (AASHTO) (2011). "Manual for bridge evaluation", 2nd Edition, *AASHTO Publications,* Washington D.C.

Federal Highway Administration (2012). "Highway bridge replacement & rehabilitation program." Washington D.C.

Transportation Research Board (2007). "Bridge inspection practices." *National Academies of Sciences, Engineering, and Medicine*. Washington, D.C. 20001.

Florida State Department of Transportation (2008). "Bridge condition terminology and inspection process", Tampa, FL.

Tang, P., Akinci, B. and Garrett Jr., J. H. (2007). “Laser scanning for Bridge inspection and management.” Improving Infrastructure Worldwide. *IABSE Symposium* Weimar, Germany. Report 93. 17–24.

Sanford, K. L., Herabat, P., Mcneil, S. (1999). “Bridge management and inspection data: leveraging the data and identifying the gaps.” proc., *Eighth transportation research board conference on bridge management*.

Chen, X.N., Xia, Q., Zhang, S.H. and Zhou, Y. (2005). "3D Laser Scanner System for Surveying and Engineering.” *Department of Photogrammetry and Remote Sensing Engineering, Zheng Zhou Institute of Survey and Mapping*, China.

Lichti, D. and Licht, M.G. (2006). "Experiences with Terrestrial Laser Scanner Modeling and Accuracy Assessment." Department of Spatial Sciences, Curtin University of Technology, Perth, WA, Australia, *Institut fur Photogrammetrie und Fernerkundung, Universitat Karlsruhe*, Karlsruhe, Germany.

Thilmany, J. (2012). “The rise of reverse engineering.” <https://www.laserdesign.com/3d-scanning-reverse-engineering-applications>. (May 1, 2017).

Cignoni, P. and Scopigno, R. (2008). "Sampled 3D models for CH applications: A viable and enabling new medium or just a technological exercise*?" ACM Journal on Computing and Cultural Heritage.* 1 (1): 1–23.

Gurjar, P. K. and Prakash, O. (2017). “The role of laser scanning technology lidar scanning and building information modelling in building construction*.” International journal of engineering sciences & research technology*, 6 (3): 317-320.

Fallon, E. (2012). “a look at 3F laser scanning in the construction industry and beyond.” <http://rhodes-group.com/newsletter/winter-2012>. (June 21, 2016).

Guldur, B. (2014). “Laser-based structural sensing and surface damage detection”, dissertation, presented to Northeastern University at Boston, MA, in partial fulfillment of the requirements for the degree of Doctor of Philosophy.

Xiong, X., Adan, A., Akinci, B., and Huber D. (2013). “Automatic creation of semantically rich 3D building models from laser scanner data,” *Automation in Construction,* 31, 325-337.

Alizadehsalehi, S., Koseoglu, O., and Celikag, M. (2015) “Integration of Building Information Modeling (BIM) and Laser Scanning in Construction Industry.” *AEI* 2015: pp. 163-174

Randall, T. (2011). "Construction Engineering Requirements for Integrating Laser Scanning Technology and Building Information Modeling." *Journal of Construction Engineering and Management* 137(10): 797-805.

Gopalakrishnan, K., Wang, T., Somani, A., Smadi, O., and Ceylan, H. (2016). “Machine-Vision-Based Roadway Health Monitoring And Assessment: Development Of A Shape-Based Pavement-Crack-Detection Approach.” *Institute of Transportation,* Iowa State University.

Golparvar-Fard, M., Bohn, J., Teizer, J., Savarese, S., and Pena-Mora, F. (2011). "Evaluation of image-based modeling and laser scanning accuracy for emerging automated performance monitoring techniques." *Automation in Construction* 20(8): 1143-1155.

Cho, Y., Haas, C., Liapi, K., and Sreenivasan. S. (2002) “A framework for rapid local area modeling for construction automation.” *Automation in Construction*, 11 (6): pp. 629–641

Eastman, C., Teicholz, P., Sacks, R., and Liston, K. (2008). BIM Handbook, *John Wiley and Sons*, Hoboken, NJ.

El-Omari, S., and Moselhi, O., (2008) “Integrating 3D Laser Scanning and Photogrammetry for Progress Measurement of Construction Work.”, Automation in Construction Journal, 18(1), 1-9

Gielsdorf, F., Rietdorf, A. and Gruendig, L. (2004). "A Concept for the Calibration of Terrestrial Laser Scanners.” *TS 26 Positioning and Measurement Technologies and Practices II-Laser Scanning and Photogrammetry*. Athens, Greece.

Prasanna, P., Dana, K. J., Gucunski, N., Basily, B. B., La, H. M., Lim R. S., and Parvardeh, H. (2014). “Automated crack detection on concrete bridges.” *IEEE Transactions on Automation Science and Engineering*, PP (99), 1–9.

La, H.M., Lim, R.S., Basily, B.B., Gucunski, N., Yi, J., Maher, A., Romero, F.A., and Parvardeh, H. (2013). “Mechatronic systems design for an autonomous robotic system for high-efficiency bridge deck inspection and evaluation.” *IEEE/ASME Transactions on Mechatronics*, 18 (6), 1655–1664.

Nishikawa, T., Yoshida, J., Sugiyama, T., and Fujino, Y. (2012). “Concrete crack detection by multiple sequential image filtering.” *Computer-Aided Civil Infrastructure* Eng., vol. 27, no. 1, pp. 29–47.

Ganapuram, S., Adams, M., and Patnaik, A. (2012). “Quantification of cracks in concrete bridge decks in Ohio district 3.” Report FHWA/OH-2012/3, Ohio department of transportation.

Brown, M., Sellers, G., Folliard, K., J., and Fowler, D. W., (2001). “Restrained Shrinkage Cracking of Concrete Bridge Decks: State-of-the-Art Review.” *Center for Transportation Research, Bureau of Engineering Research, The University of Texas at Austin*, June, pp. 1-43.

Lwin, M. M., and Russell, H. G., (2006). “Reducing Cracks in Concrete Bridge Decks.” *HPC Bridge Views, U. S. Department of Transportation, Federal Highway Administration,* Issue No. 45, pp. 1.

Zhu, Z., German, S., and Brilakis, I. (2011). “Visual retrieval of concrete crack properties for automated post-earthquake structural safety evaluation.” *Automation in Construction,* vol. 20, no. 7, pp. 874–883.

Yamaguchi T., and Hashimoto, S. (2010). “Fast crack detection method for large-size concrete surface images using percolation-based image processing.” *Machine Vision Applications,* vol. 21, no. 5, pp. 797–809.

Lee, B., Kim, Y., Yi, S., and Kim, J. (2013). “Automated image processing technique for detecting and analyzing concrete surface cracks.” *Structure Infrastructure Eng*., vol. 9, no. 6, pp. 567–577.